

ERASER: Machine Unlearning in MLaaS via an Inference Serving-Aware Approach

Yuke Hu*
Zhejiang University
yukehu@zju.edu.cn

Jian Lou*
Zhejiang University
jian.lou@zju.edu.cn

Zhan Qin†
Zhejiang University
qinzhan@zju.edu.cn

Jiaqi Liu
Zhejiang University
jiaqi.liu@zju.edu.cn

Feng Lin
Zhejiang University
flin@zju.edu.cn

Kui Ren
Zhejiang University
kuiren@zju.edu.cn

Abstract

Over the past few years, Machine Learning-as-a-Service (MLaaS) has received a surging demand for supporting Machine Learning-driven services to offer revolutionized user experience across diverse application areas. MLaaS provides inference service with low inference latency to application users based on an ML model trained using a dataset collected from numerous individual data owners. Recently, for the sake of data owners' privacy and to comply with the "right to be forgotten (RTBF)" as enacted by data protection legislation, many machine unlearning methods have been proposed to remove data owners' data from trained models upon their unlearning requests. However, despite their promising efficiency, almost all existing machine unlearning methods handle unlearning requests in a manner that is independent of inference requests, which unfortunately introduces new security and privacy vulnerabilities for machine unlearning in MLaaS.

In this paper, we propose the ERASER framework for machine unlearning in MLaaS via an inference serving-aware approach. ERASER proposes a novel certified inference consistency mechanism that reduces inference latency by selectively postponing unlearning execution incurred by unlearning requests from data owners, while strictly adhering to the RTBF principle. ERASER offers three groups of design choices to allow for tailor-made variants that best suit the specific environments and preferences of different MLaaS systems. Extensive empirical evaluations across various settings confirm ERASER's effectiveness, e.g., it can effectively save up to 99% of inference latency and 31% of computation overhead over the inference-oblivion baseline.

1 Introduction

Machine Learning (ML) has witnessed a meteoric rise in its applications across diverse areas, becoming not only ubiquitous but also essential to enhance user experience

[7, 28, 29, 54]. ML-powered applications are oftentimes supported by ML-as-a-Service (MLaaS) [1, 5, 6] on the *server* side (e.g., cloud platforms [2–4]), whereby the ML model is built on a large training dataset collected from numerous individuals (i.e., *data owners*) and then deployed to serve inference requests from application users (i.e., *queriers*). The server in MLaaS is responsible for handling requests from both queriers and data owners at the same time, with each group having its own unique requirements and concerns. For queriers, the server's primary goal is to provide timely responses to their inference requests, keeping inference latency within an acceptable limit [15, 24, 25, 27, 49, 62]. For data owners, a striking concern is the risk to their data privacy, which is susceptible to privacy attacks such as black-box membership inference attacks (MIA) [38, 39] that can determine if a training sample exists based on inference results.

Machine unlearning is a nascent privacy-respecting research field that seeks to comply with the "right to be forgotten" (RTBF) legal principle, which involves removing the corresponding data from trained ML models in response to their data owners' unlearning requests [9, 11, 23, 26, 53, 59]. It has gained increasing research attention in recent years, which is mainly prompted by the enforcement of RTBF in data protection regulations worldwide, including the European Union's GDPR [41], the California Consumer Privacy Act (CCPA) [47], and Canada's proposed Consumer Privacy Protection Act (CPPA) [8]. Most existing research on machine unlearning focus on improving the efficiency of the machine unlearning mechanism and have achieved promising acceleration over the baseline approach of retraining the ML model on the remaining dataset from scratch [9–12, 14, 19–22, 33, 40, 43, 44, 46, 48, 52, 56, 58, 60, 61, 63]. Among the many existing approaches, SISA (Sharded, Isolated, Sliced, and Aggregated) [9] is a prominent example of an exact unlearning solution that is general enough to be applied to various ML models. In addition to efficiency, some work [13, 18, 42] have also examined the security and privacy aspects of machine unlearning, revealing that new security and privacy issues can arise.

*Co-first authors

†Corresponding author

However, existing machine unlearning approaches mostly focus on the unlearning requests and consider unlearning requests separately from inference requests ¹. This inference-oblivion handling of unlearning requests oversimplifies the problem of machine unlearning in MLaaS and can even conceal potential security and privacy threats in an MLaaS environment where both types of queries exist. In fact, as will be detailed in Sect.3, we have discovered that machine unlearning in MLaaS can suffer from two new security and privacy vulnerabilities if the server uses simple strategies for scheduling unlearning and inference requests. One is the “unlearning-request-first” strategy. Upon receiving unlearning requests from data owners, the server temporarily suspends responses to inference requests to prioritize unlearning execution. While this strategy strictly adheres to the RTBF regulatory requirements, it may lead to infinite blocking of responses to normal inference requests. The other is the “inference-request-first” strategy. This approach suspends all incoming unlearning requests to prioritize responding to inference requests. Unlearning execution is then postponed until certain conditions are met. Alternatively, given adequate resources, two parallel systems can be maintained. Upon receiving an unlearning request, one system continues providing inference services using a model that hasn’t undergone unlearning execution, while the other simultaneously performs the unlearning execution in the background. Once unlearning is complete, a switch between the two systems occurs. However, such methods inherently violate the RTBF principle. After receiving an unlearning request from a data owner, the server continues to use a model containing the data owner’s information to provide inference services, thereby exposing it to potential threats like MIA even when data deletion has already been requested, leading to extra privacy risks for data owners. Both strategies are implicitly suggested by existing machine unlearning works and proposed in an inference-oblivion manner.

To address the above issues, we propose ERASER: machinE unleaRning in MLaaS via an inferencE seRving-aware approach. ERASER can reduce inference latency by conditionally postponing unlearning execution through a certified inference consistency mechanism. The method for determining whether postponing unlearning execution will incur privacy risks in the second simple strategy involves distinguishing whether the model’s response to an inference request after unlearning execution differs from that of a model retaining the sensitive data. This is because such discrepancies indicate that the sensitive data has a significant impact on the model, making it extremely susceptible to MIA that can potentially identify the data. Unlearning execution can only be postponed when it’s ensured that the server’s response to inference requests remains consistent before and after the unlearning execution. However, verifying this consistency by directly executing the

¹Upon the submission of this work, we find a concurrent work on arXiv which also studies machine unlearning under the MLaaS setting [31]. However, we study different problems under this setting.

unlearning process is meaningless. Therefore, we exploit the inherent structural characteristics of SISA to design a certified inference consistency mechanism. This mechanism can anticipate whether the prediction outcome would change after unlearning execution. If deemed consistent, denoting certified prediction consistency, the unlearning execution can be postponed, allowing for an immediate response to the current inference request. All postponed unlearning executions can be batch-processed, thereby reducing processing time and computational resource consumption without introducing additional privacy risks, ultimately enhancing the response speed to inference requests.

Considering the diverse resources and preferences of different servers, we offer three groups of design options under the ERASER framework: the capability to simultaneously maintain both training and inference environments, the timing for executing unlearning execution, and the handling strategy for inference requests that cannot achieve consistency. Based on these options, we have designed seven distinct methods. Servers can choose the appropriate method based on their preferences regarding response speed, resource consumption, and privacy protection.

- To the best of our knowledge, we are the first to identify the security and privacy vulnerabilities of machine unlearning in the MLaaS setting, resulting from two simplified strategies suggested by existing inference-oblivion machine unlearning works.
- We propose ERASER, a new machine unlearning framework for MLaaS developed in an inference serving-aware manner, which can reduce inference latency while avoiding security and privacy vulnerabilities.
- We further propose seven variants under ERASER based on three design options, each being tailor-made to specific environments and preferences of different MLaaS systems.
- We perform a comprehensive evaluation on four machine learning models using four real-world datasets to assess the performance of ERASER. The results demonstrate that ERASER and its variants significantly reduce inference latency and computational overhead compared to the inference-oblivious baseline in different settings, achieving up to 99% saving in inference latency and 31% saving in computation overhead.

2 Background and Preliminary

2.1 MLaaS

Most existing MLaaS have two phases: the model training phase and the inference serving phase. Since the two phases have different design objectives and resource preferences, the training and inference contexts are usually optimized and

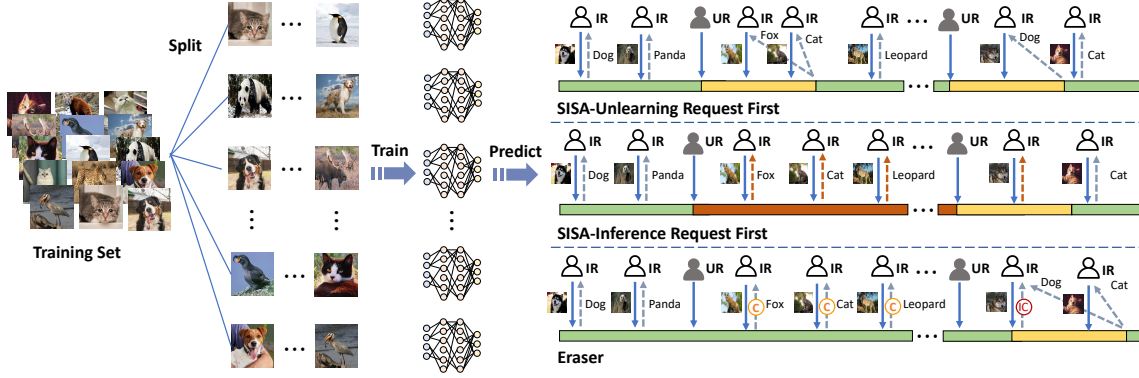


Figure 1: Illustration of comparison between ERASER and SISA with two inference-oblivion strategies. Green represents inference service without privacy risk, red indicates inference with privacy risk, and yellow signifies unlearning execution.

maintained separately. In this paper, we focus on the general classification model in a fully supervised learning setting, which is fundamental and widely adopted in applications.

ML model and training. ML model $F_{\theta} : \mathcal{X} \rightarrow \mathbb{Y}$ with model parameters θ maps from the feature space \mathcal{X} to the discrete label set \mathbb{Y} based on the training dataset \mathcal{D} . The training dataset $\mathcal{D} = \{(\mathbf{x}_1, y_1), \dots, (\mathbf{x}_N, y_N)\}$ is collected from N data owners, where for each $i \in \{1, \dots, N\}$, $\mathbf{x}_i \in \mathcal{X}$ and $y_i \in \mathbb{Y}$ are data owner i 's feature and label. F_{θ} takes the empirical risk minimization form $F_{\theta} = \frac{1}{N} \sum_{i=1}^N l_{\theta}(\mathbf{x}_i, y_i)$, where $l_{\theta}(\mathbf{x}_i, y_i)$ is the loss function on each individual (\mathbf{x}_i, y_i) . The objective of the ML training phase is to find the optimal θ^* to minimize the overall loss on the training dataset, i.e., $\theta^* := \arg \min_{\theta} \{F_{\theta} = \frac{1}{N} \sum_{i=1}^N l_{\theta}(\mathbf{x}_i, y_i)\}$. The training phase is an offline process that can require significant computation, sometimes taking hours or even days to train a model from scratch.

ML inference and inference serving. Given the trained ML model, the ML inference takes an inference sample $\mathbf{z} \in \mathcal{X}$ and provides the inference result by $F(\mathbf{z}) = y \in \mathbb{Y}$ (for notational convenience, we will omit θ from $F_{\theta}(\mathbf{z})$ in the sequel). The inference serving of MLaaS has the primary objective to deliver timely inference results to application users. The inference phase is an online/interactive process focused on achieving low inference latency. It is a challenging problem to balance response time with cost and resource effectiveness under dynamic workloads and fluctuating resource availability. Many approaches have been proposed that can achieve promising frontiers among inference latency and cost/resources effectiveness [15, 25, 49, 62].

2.2 Machine Unlearning

Machine unlearning is the task to remove a specific training sample from the trained ML model upon its data owner's unlearning request. The most basic yet inefficient approach is "retraining-from-scratch", which retrains the ML model on the remaining training set (i.e., the original training set excluding the sample to be unlearned) from scratch. To avoid the

prohibitive computational cost of "retraining-from-scratch", many efficient machine unlearning mechanisms have been proposed, which can be roughly categorized into exact unlearning mechanisms [9–12, 14, 19, 35, 52, 56, 61] and approximate unlearning mechanisms [20–22, 33, 40, 43, 44, 46, 48, 58, 60, 63]. Exact machine unlearning mechanisms produce models identical to the one produced by "retraining-from-scratch", therefore capable of completely removing the requested data. Approximate unlearning mechanisms, on the other hand, trade exactness in data removal for improved computational and memory efficiency.

SISA. In this paper, we focus on a notable exact unlearning mechanism called SISA [9], which is known for its ability to completely remove data and its generality to be applicable to various common ML models. During training, SISA divides the training dataset into multiple shards and builds a constituent model on each shard. Inference results are obtained by aggregating answers from all constituent models. During unlearning, only the shard containing the data to be unlearned is retrained to update the corresponding constituent model.

3 Problem Definition and Motivating Threats

In this section, we first introduce the threat model of machine unlearning in MLaaS in Sec.3.1. Then, we present two toy attacks that pose new security and privacy threats to machine unlearning in MLaaS in Sec.3.2. These attacks motivate our design goals, which are discussed in Sec.3.3.

3.1 Threat Model

There are three parties in machine unlearning in MLaaS: data owners, queriers, and the server.

Data owners and unlearning requests. Data owners contribute their personal data to the server to facilitate the training of ML models. As granted by the "right to be forgotten" legislation, data owners have the right to request the removal of their data from the server to protect their privacy. After the

ML model is trained and deployed in MLaaS, data owners can submit unlearning requests at any time. In response to an unlearning request, the server executes the machine unlearning mechanism to unlearn the relevant data from the trained model. Some data owners can have malicious purposes for submitting unlearning requests, such as attempting to increase the response time for inference requests, rather than genuinely seeking to protect their privacy. Furthermore, these malicious data owners may collude to coordinate the submission timing of unlearning requests in an attempt to cause the greatest possible inference latency. However, we do not take into account fake unlearning requests. Instead, we assume that all unlearning requests submitted to the server are from legitimate data owners whose data has been used in model training.

Queriers and inference requests. Queriers are users of the application supported by MLaaS. After the ML model is trained and deployed, queriers can submit inference requests to the server at any time and receive the inference result from the server. The time it takes from submitting the request to receiving the results is known as the inference latency or response time. Ideally, queriers want the inference latency to be as short as possible to minimize their wait time. In reality, if the inference latency exceeds an acceptable limit, queriers may abandon the service provider due to poor user experience and the delayed responses may cease to be useful [25, 27, 29]. Some queriers can have malicious purposes for submitting inference requests. Among the various widely recognized malicious inference threats, a prominent example is the privacy attack [32, 38, 39, 51, 55], in which queriers attempt to steal sensitive information pertaining to targeted data owners based on the inference results.

Server. In this paper, the server represents service provider(s) offering MLaaS, which can be supported by cloud platforms. The server operates in two phases in existing MLaaS literature. During the training phase, the server builds the ML model using the training dataset that contains personal and potentially sensitive information from data owners. During the inference serving phase, the server processes queriers' inference requests by feeding the inference sample to the ML models and returning the inference result to the querier. To adhere to the “right to be forgotten” mandate enforced by data protection regulations, the server further takes into account unlearning requests from data owners during the inference serving phase. The server processes the unlearning request by executing the machine unlearning mechanism to remove the unlearning requester's data from the deployed model. We assume that the server is honest and will faithfully carry out all three of its designated functions discussed above, namely training, inference, and machine unlearning.

3.2 Two Motivating Threats on Machine Unlearning in MLaaS

To begin with, we demonstrate that machine unlearning in MLaaS is susceptible to new security and privacy vulnerabilities if unlearning requests are handled in an inference-oblivion manner. Specifically, we present two toy attacks that target two simplistic strategies for processing unlearning requests. Both strategies are inference-oblivion and implicitly suggested by existing machine unlearning literature, in the name of single data removal and batch removal, respectively. One toy attack will cause the inference latency to become infinitely long, effectively rendering the normal inference service unusable, while the other will cause extra privacy risks for data owners whose unlearning requests should have been processed earlier.

Security threat: Blocking inference requests. In the first strategy for processing unlearning requests, the server immediately executes the machine unlearning mechanism for every incoming unlearning request, a.k.a., “unlearning-request-first” strategy, as illustrated in the top row of Figure 1. Meanwhile, all inference requests submitted while the machine unlearning mechanism is executing have to be delayed until the server completes the unlearning update and deploys the new model for inference service once again.

The toy attack targeting the “unlearning-request-first” strategy can infinitely block the processing of inference requests, ultimately preventing the server from providing any normal inference services. The attack is carried out by adversarial data owners who initially provide data to the server for model training. Once the model is trained and the inference and unlearning services are online, they periodically submit unlearning requests to the server to demand one of their data be unlearned. In an extreme and simplified scenario, they submit successive unlearning requests at intervals equal to the time it takes for the server to complete one machine unlearning process. As a result, all inference requests submitted at any time are blocked by these malicious unlearning requests. In fact, it suffices for the attack to cause the inference time to exceed an acceptable response time in order to disrupt normal inference services, rather than infinitely blocking the inference requests.

Privacy threat: Introducing extra privacy risk. In the second strategy for processing unlearning requests, the server does not process the pending unlearning requests until a certain number of the unlearning requests have accumulated or a predefined waiting time has been reached. Meanwhile, the server continues processing incoming inference requests immediately based on the old model, a.k.a., “inference-request-first” strategy, as illustrated in the middle row of Figure 1. It has the smallest extra inference latency for inference requests submitted before executing the next machine unlearning mechanism for pending unlearning requests.

The toy attack targeting the “inference-request-first” strategy has the potential to introduce extra privacy risks for data

owners having submitted normal unlearning requests. The attack is carried out by adversarial queriers who attempt to infer privacy information of a targeted unlearning requester’s data by submitting malicious inference requests to the server. Because of the “inference-request-first” strategy, the target’s data is not unlearned from the model under inference servicing until the next scheduled unlearning execution. Malicious inference requests processed during this time give the attacker an extra advantage in better stealing the target data’s privacy.

3.3 Desiderata for Unlearning in MLaaS

The above two motivating threats underscore the importance of developing an inference serving-aware machine unlearning framework in the MLaaS setting. In this setting, the server is responsible for cautiously scheduling the processing of inference and unlearning requests to minimize inference latency and extra privacy risks, as illustrated in the bottom row of Figure 1. In detail, we have the following two design goals for the server.

Low inference latency: For MLaaS admitting unlearning requests, the inference latency can be increased by the unlearning process for two reasons: 1) Executing the machine unlearning mechanism takes much longer than executing an inference sample; 2) The subsequent inference requests may have to wait until the ML model complete the unlearning update. Therefore, the server’s first design goal is to minimize the extra inference latency caused by unlearning executions for as many inference requests as possible. One way to reduce extra inference latency is by selectively postponing the process of certain unlearning requests. This has two benefits: 1) subsequent inference requests can be processed without waiting for unlearning execution; 2) multiple unlearning requests can be processed by executing a single machine unlearning mechanism, curtailing the total time spent on unlearning.

Avoid extra privacy risk: Achieving the first design goal above may increase the privacy risk for the personal data of unlearning requesters. If an unlearning request is postponed behind a sequence of inference requests, the unlearning requester’s data remains in the ML model and may be subject to information leakage from predictions made on the yet-to-be-unlearned model. To prevent this, the server’s second design goal is to ensure that the postponed unlearning requests do not increase the privacy risk for their requesters.

There are also other opportunities for improvement in both security and efficiency of machine unlearning scheme. However, these areas are orthogonal to the research presented in this paper. Further details can be found in Appendix A

4 ERASER: Machine Unlearning in MLaaS

Motivated by the security and privacy vulnerabilities and design goals in the preceding section, we propose ERASER, a new

framework that takes an inference serving-aware approach to machine unlearning in MLaaS.

4.1 Intuition and Overview

Intuition. As mentioned in the first design goal, we can reduce inference latency by selectively postponing the execution of certain unlearning requests and processing subsequent inference requests first. Despite the benefit of reducing inference latency, we need to ensure that privacy attackers do not gain extra advantage from unlearning requesters whose data are not immediately unlearned. At first glance, the key to the server’s design is selecting the right unlearning requests to postpone. Rather, we can take a complementary (but conceptually equivalent) view by selecting from subsequent inference requests that can be answered before executing the pending unlearning requests. The basic principle is to select inferences having consistent inference results with or without machine unlearning of the pending unlearning requests. This way, a black-box privacy attacker cannot gain any extra advantage in stealing the unlearning requester’s data based on the inference results. Otherwise, if the inference result is inconsistent, which means the result can be significantly influenced by the to be unlearned sensitive data, it cannot be sent to the querier without first processing the unlearning request

With this selection principle, the challenge is how to certify that the inference result is consistent on models with and without machine unlearning of the pending unlearning requests. Apparently, it is infeasible to compare the inference results by actually executing machine unlearning, as this would defeat our goal of avoiding its execution in the first place. To certify inference consistency without actual machine unlearning execution, we resort to the concept of model robustness with respect to small changes in the training dataset [34, 37, 57]. Roughly speaking, this refers to the property that two ML models trained on neighboring datasets (i.e., two datasets that have most of the data in common except a few) have the same inference results. This naturally evokes the idea of utilizing Differential Privacy (DP) techniques for model training. However, the primary challenge with the DP-based approach is that the robustness offered by DP allows only for approximate unlearning, rather than exact unlearning. Additionally, the noise introduced by DP can significantly decrease the model’s utility. The ideal robustness entails two favoring consequences: 1) more subsequent inference requests can be responded to before the machine unlearning the pending unlearning requests, reducing waiting time; 2) more unlearning requests can be accumulated and executed all at once by a single unlearning execution, reducing unlearning execution time.

Finally, we arrive at the two concrete questions to be answered: 1) How to convert any ML models to a more robust counterpart in a generally applicable way that is also compatible with one of the existing machine unlearning mechanisms;

2) How to connect the robustness concept with the inference consistency to certify that certain inference requests can be responded without actual machine unlearning of the pending unlearning requests.

Overview of ERASER. Taking on the above intuition, we propose the ERASER framework with two phases, i.e., the training phase and the inference&unlearning serving phase, where the latter supports both inference and unlearning requests.

During the training phase, ERASER is given the training dataset, the model architecture and loss designated by the application. Then, ERASER employs the same training strategy as SISA, dividing the training dataset into K shards and building each constituent model independently on its shard. As will be shown in Sec.4, this shard-aggregate strategy makes the model more robust to small changes in the training dataset (i.e., the small amount of unlearned data in our context), in addition to its known unlearning efficiency from the original SISA paper. In this sense, ERASER uncovers a hidden benefit of SISA when applied to machine unlearning in MLaaS.

During the inference and unlearning serving phase, ERASER serves both inference requests from queriers and unlearning requests from data owners. It aims to avoid frequent interruptions of normal inference service by executing unlearning requests. For an incoming unlearning request, ERASER records it and the shard it belongs to but does not necessarily execute the machine unlearning immediately (i.e., treats it as a pending unlearning request). ERASER will keep the data and shard index for all pending unlearning requests until they are machine unlearned. For an incoming inference query, ERASER derives a certified inference consistency mechanism to determine if the inference result will be consistent with or without machine unlearning of all pending unlearning requests. If the inference has consistent results, ERASER immediately returns the inference result to the querier. The computation of the certified inference consistency mechanism essentially involves processing the inference request itself plus some simple counting and comparing operations, with no actual machine unlearning execution. In this case, ERASER therefore incurs minimal additional inference latency caused by machine unlearning. Otherwise, if the certified inference consistency condition is not met, ERASER may need to halt the inference service and execute the machine unlearning first. However, due to the shard-aggregate strategy and increased robustness, a large portion of inference requests have certified inference consistency and can be immediately responded to, as will be shown in the empirical results.

In Sec.4.2, we provide a formalization of ERASER. In Sec.4.3, we derive the certified inference consistency mechanism. In Sec.5.3, we analyze ERASER in terms of inference waiting time to show its advantage compared to the inference-oblivion baseline approach SISA.

4.2 Formalization of ERASER

Based on the overview, we formalize the three key functions (i.e., training, inference, and unlearning) in the two phases of ERASER below.

Training. To facilitate unlearning, ERASER builds the model F by shard-and-aggregate strategy following SISA. First, it randomly divides the training dataset \mathcal{D} into K shards $\mathcal{S}_1, \dots, \mathcal{S}_K$. On each shard \mathcal{S}_k , ERASER trains a constituent model f_k , which will result in K constituent models $\{f_1, \dots, f_K\}$.

Inference. Denote an inference request by $q = (\mathbf{z}, 'Inference')$. Each constituent model provides prediction class $y_k = f_k(\mathbf{z})$ on the inference request sample \mathbf{z} . To provide the final inference result $F(\mathbf{z})$, ERASER aggregates the prediction results from all K constituent models by majority voting. That is, ERASER counts the number of constituent models that has inference result y for each candidate label $y \in \mathbb{Y}$, given by

$$\text{Count}_y(\mathbf{z}) := |\{k \in [K] \mid f_k(\mathbf{z}) = y\}|. \quad (1)$$

The final inference result $F(\mathbf{z})$ is the label that has the largest count, given by

$$F(\mathbf{z}) := \arg \max_{y \in \mathbb{Y}} \text{Count}_y(\mathbf{z}), \quad (2)$$

where ties are broken by returning the label with a smaller index.

Unlearning. Denote an unlearning request by $u = (i, 'Unlearn')$, which is sent by the i -th data owner to request for unlearning his/her data (\mathbf{x}_i, y_i) from the trained ML model. ERASER keeps track of all pending unlearning requests. At timestamp t , for any shard $k \in \{1, \dots, K\}$, let τ_k^0 be the timestamp of the most recent training/unlearning execution, \mathcal{S}_k^0 be the remaining data partition of the k -shard at timestamp τ_k^0 , f_k^0 be the ML model obtained by executing the machine unlearning mechanism on \mathcal{S}_k^0 . In other words, \mathcal{S}_k^0 has no pending unlearning requests since they have been machine unlearned at τ_k^0 to obtain f_k^0 . Then, from the most recent unlearning execution timestamp τ_k^0 to the current timestamp t , we denote the set of pending unlearning requests (if any) during this period by $U_k^t := \{u_k^{p_1}, \dots, u_k^{p_t}\}$. Let $\mathcal{S}_k^t := \mathcal{S}_k^0 \circ u_k^{p_1} \dots \circ u_k^{p_t}$ be the k -th shard with all pending unlearning requests U_k^t removed from \mathcal{S}_k^0 . In addition, we define f_k^t to be the constituent model that would have been machine unlearned at t on \mathcal{S}_k^t to process U_k^t . Collecting all K shards, we have $U^t := (U_1^t, \dots, U_K^t)$, $\mathcal{D}^0 = \mathcal{S}_1^0 \cup \mathcal{S}_2^0 \cup \dots \cup \mathcal{S}_K^0$, $\mathcal{D}^t = \mathcal{S}_1^t \cup \mathcal{S}_2^t \cup \dots \cup \mathcal{S}_K^t$, and $\tau^0 := (\tau_1^0, \dots, \tau_K^0)$. Correspond-

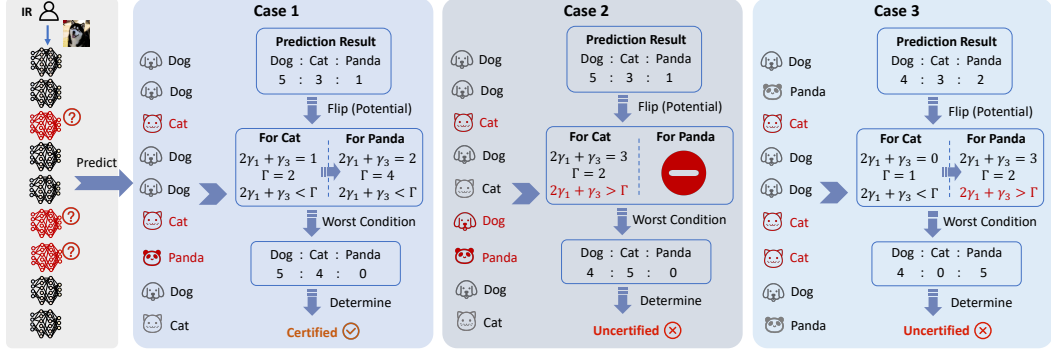


Figure 2: Illustration of three representative cases for the certified inference consistency mechanism.

ingly, we introduce the following notations,

$$\text{Count}_y^0(\mathbf{z}) := |\{k \in [K] \mid f_k^0(\mathbf{z}) = y\}|, \quad (3)$$

$$\text{Count}_y^t(\mathbf{z}) := |\{k \in [K] \mid f_k^t(\mathbf{z}) = y\}|; \quad (4)$$

$$F^0(\mathbf{z}) := \arg \max_{y \in \mathbb{Y}} \text{Count}_y^0(\mathbf{z}), \quad (5)$$

$$F^t(\mathbf{z}) := \arg \max_{y \in \mathbb{Y}} \text{Count}_y^t(\mathbf{z}). \quad (6)$$

From τ^0 to t , ERASER responds to inference requests based on the old model F^0 , which calls for certified inference consistency to avoid extra privacy risks, as presented below.

4.3 Certified Inference Consistency

Definition of inference consistency. According to the threat model, the adversary can only access the final inference results (i.e., $F^0(\mathbf{z})$). Thus, the postponed unlearning will not cause extra privacy risks if $F^0(\mathbf{z}) = F^t(\mathbf{z})$, i.e., the inference results on \mathbf{z} are consistent between the model without timely unlearning (F^0) and the model if unlearning were executed (F^t). Under this inference consistency condition, the inference request on \mathbf{z} can be immediately responded to the querier without the actual machine unlearning to obtain F^t at timestamp t . The following definition formalizes the inference consistency for machine unlearning in MLaaS.

Definition 1 (Inference Consistency). For the inference request on sample \mathbf{z} , the MLaaS has inference consistency between the ML models with and without processing the pending unlearning requests, if they have the same prediction results on \mathbf{z} . That is, it has $F^0(\mathbf{z}) = F^t(\mathbf{z})$, where F^0 is the model without U^t unlearned and F^t is the model with actual unlearning, as specified in eq.(5) and eq.(6), respectively.

Certified inference consistency. It is infeasible in practice to exactly check the condition in Definition 1, because one has to execute the machine unlearning mechanism to obtain f_1^t, \dots, f_K^t in the first place. Rather, we need to certify the

inference consistency based on the prediction results made by f_1^0, \dots, f_K^0 and the records of pending unlearning requests. For this purpose, we derive Theorem 1 to provide a certification condition under which inference consistency will hold, while neglecting the need to unlearning-update f_1^t, \dots, f_K^t . The rationale behind Theorem 1 is by first constructing the case that can lead to inference inconsistency and then providing the certification condition to avoid such undesired case. Consequently, as long as the certification condition in Theorem 1 holds, we can ensure the certified inference consistency without the actual machine unlearning.

Theorem 1 (Certified Inference Consistency). Suppose that the most recent unlearning-updated training dataset is \mathcal{D}^0 , the pending unlearning requests are U^t , and the shards with pending unlearning requests are $\{k \in [K] \mid S_k^t \neq S_k^0\}$. Given inference sample \mathbf{z} , let y_a be the labels having maximum counts among $\text{Count}_y^0(\mathbf{z})$ made by $f_1^0(\mathbf{z}), \dots, f_K^0(\mathbf{z})$ and y_b is a label different from y_a , i.e., $\forall y_b \in \mathbb{Y}, y_b \neq y_a$. Let the counts $\gamma_1, \gamma_2, \gamma_3$ be defined as

$$\gamma_1 := |\{k \in [K] \mid S_k^t \neq S_k^0 \wedge f_k^0(\mathbf{z}) = y_a\}|; \quad (7)$$

$$\gamma_2 := |\{k \in [K] \mid S_k^t \neq S_k^0 \wedge f_k^0(\mathbf{z}) = y_b\}|; \quad (8)$$

$$\gamma_3 := |\{k \in [K] \mid S_k^t \neq S_k^0 \wedge f_k^0(\mathbf{z}) \neq \{y_a, y_b\}\}|. \quad (9)$$

Then, ERASER has certified inference consistency for the inference request on \mathbf{z} , if the following condition holds: $\forall y_b \in \mathbb{Y}, y_b \neq y_a, 2\gamma_1 + \gamma_3 \leq \Gamma$, where $\Gamma = \max_{\forall y_b \in \mathbb{Y}, y_b \neq y_a} \{\text{Count}_{y_a}^0(\mathbf{z}) - \text{Count}_{y_b}^0(\mathbf{z}) - \mathbb{1}(y_b < y_a)\}$ with $\mathbb{1}(\cdot)$ being the indicator function. In other words, the inference request on \mathbf{z} can be responded to its querier immediately without incurring extra privacy risk while avoiding the need to remove U^t from \mathcal{D}^0 and wait for the unlearning update to obtain $f_1^t(\mathbf{z}), \dots, f_K^t(\mathbf{z})$.

The proof is relegated to Appendix B.1. Figure 2 provides an illustration for three cases that have different results from the inference consistency certification mechanism.

Theorem 1 draws inspiration from the certified robustness defense against data poisoning attacks [34, 37, 57]. However,

as demonstrated in Appendix B.2, straightforwardly applying the certified robustness from [37] results in a worse certification condition. In other words, ERASER would no longer certify on inference samples it should have. In fact, Theorem 4 in Appendix B.2 can be regarded as having the certification condition $2\gamma_1 + 2\gamma_2 + 2\gamma_3 \leq \Gamma$, which is apparently more strict than ours $2\gamma_1 + 0\gamma_2 + 1\gamma_3 \leq \Gamma$. As a result, our certification analysis is tailored to the machine unlearning in MLaaS problem and achieves a more fine-grained certification condition.

5 Design Options and Variants of ERASER

In this section, we further explore several specific variations within the ERASER framework, differentiated by three groups of design options. Our goal is to examine three key design choices to highlight the challenges and research opportunities presented in this emerging problem of machine unlearning in MLaaS. While there are numerous other design considerations, questions, and choices that cannot be comprehensively investigated in a single paper, these are equally important and can be explored in future work.

5.1 Design Options

Design option I: maintain single or double contexts. We consider whether to have both inference and unlearning contexts or not. In existing MLaaS literature, it is widely recognized that the training and inference contexts have distinct characteristics. For instance, the training context involves loading the training dataset and is typically an offline computation, while inference is interactive and requires low latency. Thus, these two contexts are often studied and optimized separately. However, the emerging need for machine unlearning blurs the boundary between training and inference. Machine unlearning mechanisms share characteristics with both training and inference: on one hand, they require (partial) training data and more computation than inference, resembling training; on the other hand, they are interactive and require careful scheduling to avoid additional inference latency.

- *Design Option I-A:* ERASER opts to maintain both the inference context at the front end and the unlearning context at the back end, with dedicated resources at both ends that can operate in parallel. The former utilizes all older copies of the constituent models to provide inference service with certified inference consistency. The latter executes the unlearning mechanism to update the corresponding constituent models that have pending unlearning requests to process.
- *Design Option I-B:* ERASER opts to maintain only one context at a time and switches between contexts when processing different types of requests. When switching to the unlearning context, it halts all inference requests until the unlearning update is complete.

Design Option II: Timing of unlearning. We explore when to execute the pending unlearning requests and provide three options below depending on whether the unlearning requests are processed immediately or waiting until there are inference requests that cannot satisfy the prediction consistency condition.

- *Design Option II-A:* ERASER opts to accumulate unlearning requests until an inference request fails to meet the certified inference consistency condition. At that point, all pending unlearning requests are machine unlearned together. In the meantime, subsequent inference requests can only be responded to if the inference sample meets the inference consistency certification based on the old model copies. This option is referred to as *uncertification-triggered unlearning*.
- *Design Option II-B:* ERASER opts to immediately execute unlearning at the back end, while serving the inference requests based on the old copies of the constituent models in the front end. The inferences without consistency need to wait for the completion of ongoing unlearning execution. This option is referred to as *immediate unlearning*.
- *Design Option II-C:* When combined with *Option III-C* introduced below, ERASER opts to execute unlearning when the uncertification ratio is reached. This option is referred to as *threshold-triggered unlearning*.

These options all have their advantages and disadvantages. Option II-A&C have a better chance of accumulating more pending unlearning requests and processing them with a single unlearning update. However, the unlearning update may occur during periods of heavy inference request workload, potentially impacting the user experience if many inference samples cannot meet the inference consistency certification and the unlearning-updated model cannot be deployed quickly enough. Option II-B can improve resource utilization for the unlearning context and complete the unlearning update earlier. However, it may also result in wasted computational resources in certain situations, such as when an earlier unlearning request could have been processed together with a later request submitted to the same shard. In future work, we will explore more sophisticated design options for unlearning timing that take multiple factors, such as workload, resource utilization, user satisfaction, and service cost, into holistic consideration.

Design Option III: Handling of uncertified inference requests. We consider how to handle uncertified inference requests under the setting of *Design Option II-C*. In conventional MLaaS that only deals with inference requests, the system design and computational resources are typically capable of handling the majority of inference requests and meeting the service-level objective (SLO) of response time. However, a small portion of them, known as tail inference requests [16, 17, 24], can be difficult to meet the SLO due to various factors raised in the practical serving environment.

There are several options to handle such tail inference requests. One option is to consider scaling up with more computational resources at the expense of higher costs. Another is to discard a small portion of them (based on a predetermined discarding ratio) when the server finds that either the inference latency will exceed an acceptable limit or the cost for additional resources is too high.

As observed in our empirical results in Sec. 6, a new factor in ERASER will cause the phenomenon of tail inference requests, i.e., failure to certify the inference consistency. This means that while most inference requests can certify inference consistency and be immediately responded to, a small portion cannot and may experience much longer inference latency as they may need to wait for the machine unlearning execution. To handle such uncertified inference requests, we propose the third design option below.

- *Design Option III-A:* ERASER opts to immediately provide the uncertified inference results to the queriers as long as such responses are within a predetermined small ratio (uncertification ratio), introduced in the same spirit as the discarding ratio.
- *Design Option III-B:* ERASER opts to store the uncertified inference requests and reprocess them with the new model after the next machine unlearning execution.

For Option III-A, the advantage is that the inference latency for uncertified inference requests that are immediately responded to can be significantly reduced. However, the downside is that these uncertified inference results introduce additional privacy risks. As such, we suggest adopting this option with more caution, e.g., by setting a very small uncertification ratio to limit the privacy risk.

5.2 Variants of ERASER

We propose seven variants with different combinations of choices for three options. The details of these choices are shown in Table 1, and a comparison among the double-context variants is presented in Figure 3. A more detailed description and comparison can be seen in Appendix D.

- *Double Contexts for Immediate Unlearning with Postponed Certified Inference (DIMP):* It corresponds to Option A-B-B, and offers low inference latency at the cost of high computation overhead.
- *Single Context for Uncertification-Triggered Unlearning with Postponed Certified Inference (SUTP):* It corresponds to Option B-A-B, and saves computation overhead compared to DIMP at the cost of increased inference latency.
- *Double Contexts for Uncertification-Triggered Unlearning with Postponed Certified Inference (DUTP):* It corresponds to Option A-A-B. This variant reduces inference latency

compared to SUTP while consuming more resources by maintaining double contexts simultaneously.

- *Single Context for Threshold-Triggered Unlearning with Uncertified Inference (STTU):* It corresponds to Option B-C-A, and introduces potential privacy risk in exchange for better inference latency and computation overhead.
- *Double Context for Threshold-Triggered Unlearning with Uncertified Inference (DTTU):* It corresponds to Option A-C-A, which differs from STTU by maintaining both contexts to reduce inference latency.
- *Single Context for Threshold-Triggered Unlearning with Postponed Certified Inference (STTP):* It corresponds to Option B-C-B. This variant saves more computation overhead than STTU, but at the cost of higher inference latency.
- *Double Context for Threshold-Triggered Unlearning with Postponed Certified Inference (DTTP):* It corresponds to Option A-C-B, and requires more resources in exchange for better inference latency compared with STTP.

Table 1: Summary of Variants under Different Design Options

Variants \ Options	I	II	III
DIMP	A	B	B
SUTP	B	A	B
DUTP	A	A	B
STTU	B	C	A
DTTU	A	C	A
STTP	B	C	B
DTTP	A	C	B

These different variants achieve a tradeoff between privacy, resource consumption, and inference latency. All double-context variants consume more resources to reduce inference latency. DIMP has the lowest inference latency among all variants, but its computation overhead is the highest. The computation overhead of DTTP is the lowest, but its inference latency is the highest. The inference latency and computation overhead of DUTP is between the first two variants. The inference latency of DTTU is close to that of DUTP, but the computation overhead is lower, at the cost of introducing privacy risk. Ultimately, the choice of variant depends on the specific requirements and constraints of a given application, such as the importance of privacy, computational resources, and response time.

5.3 Analysis

We take DIMP (Options A-B-B) and SISA with “unlearning-request-first” strategy (Options B-B-B) as examples to theoretically analyze the acceleration capability of ERASER.

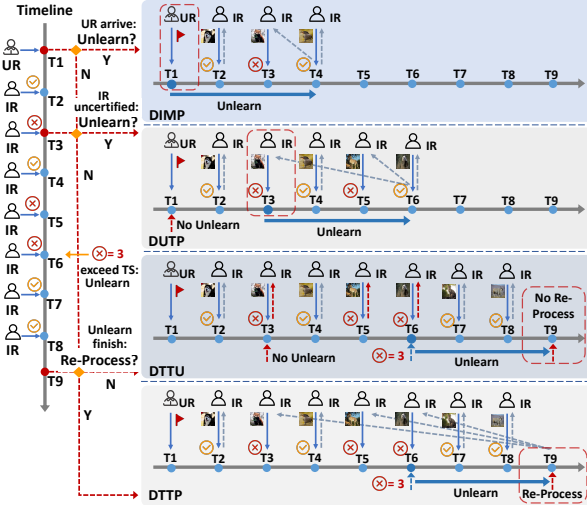


Figure 3: Illustration of variants with double contexts of ERASER.

Assume the time required to retrain a constituent model is fixed at r , the number of unlearning requests is n_u , the number of inference requests is n_i , the arrival time interval for all requests is $[0, T]$.

Theorem 2 (Waiting Time of SISA). *The expected waiting time of each inference request in SISA is*

$$\mathbb{E}(w_{sisa}) = \begin{cases} \frac{n_u r^2}{2T}, & r \leq \frac{T}{n_u} \\ r - \frac{T}{2n_u}, & r > \frac{T}{n_u} \end{cases} \quad (10)$$

Theorem 2 shows that $\mathbb{E}(w_{sisa})$ is positively correlated with the density of unlearning requests $\frac{n_u}{T}$ and the retraining time r , which is consistent with intuition.

Theorem 3 (Waiting Time of DIMP). *Assuming that the probability of the prediction result being uncertified at each judgement is p_{uc} , the upper bound of the expected inference request waiting time in DIMP is:*

$$\mathbb{E}(w_{dimp}) \leq \begin{cases} p_{uc} \cdot \frac{n_u r^2}{2T}, & r \leq \frac{T}{n_u} \\ p_{uc} \cdot (r - \frac{T}{2n_u}), & r > \frac{T}{n_u} \end{cases} \quad (11)$$

Since the actual expression of $\mathbb{E}(w_{dimp})$ can hardly be simplified into a more intuitive form (details can be seen in Appendix B.4), we give its theoretical upper bound here. The form of this upper bound is very similar to the expression of $\mathbb{E}(w_{sisa})$ in Theorem 2, which can be rewritten as $\mathbb{E}(w_{dimp}) \leq p_{uc} \cdot \mathbb{E}(w_{sisa})$. This expression shows that the processing speed of DIMP is at least $\frac{1}{p_{uc}}$ times that of SISA.

Our experimental results indicate that the p_{uc} value is typically less than 0.01, meaning that the waiting time for DIMP does not exceed 1% of SISA.

6 Experiments

In this section, we conduct experiments to answer the following research questions: **RQ1**: Can ERASER reduce the inference latency of MLaaS and computational overhead while satisfying the unlearning guarantee? **RQ2**: How do various groups of parameters affect the performance of ERASER, including 1) the hyper-parameter settings in ERASER: the number of shards and threshold of uncertification ratio; 2) frequency of requests: the density of requests per time slot and the ratio between the two types of requests; 3) server computing capability: the parallel capacity specifying the number of constituent models that can be unlearning-updated in parallel? **RQ3**: How does the temporal distribution of inference requests and unlearning requests affect the performance of ERASER?

Table 2: Details of Datasets and Models

Dataset	Dimension	Size	Classes	Architecture
MNIST [36]	28×28	60000	10	2 Conv. + 2 FC
Purchase [50]	600	250000	2	2 FC layers
SVHN [45]	$32 \times 32 \times 3$	604833	10	Wide ResNet-1-1
Imagenette [30]	$500 \times 500 \times 3$	13394	10	ResNet-18

6.1 Experiment Setup

Datasets & Models. We evaluate our ERASER on four open benchmark datasets and four common model architectures, aligning with mainstream settings, as summarized in Table 2. The datasets exhibit diversities in input dimensions, data volume, and the number of classes, while the models have different structures and parameter quantities.

Baseline Method. We take SISA with the unlearning-request-first strategy as the baseline. This variant is modified from the original SISA to satisfy the unlearning guarantee in the MLaaS scenario, as described in Sec.3.2.

Implementation Details. 1) Training: in the experiment, we first follow the SISA [9] method to divide the training set into multiple shards and then train constituent models separately using the data of each shard. The same models are served for all methods to ensure fairness. 2) Inference: the models are deployed on the server side to respond to requests. We then randomly generate 500 unlearning requests and a certain number of inference requests, with the number of inference requests determined by a hyper-parameter. These requests are randomly submitted to the server within a time interval, the length of which is dictated by a predefined density parameter. The same requests are fed to all methods for fairness. 3) Unlearning mechanism: once an unlearning update is triggered, all variants retrain the constituent models with updated data shards.

Evaluation Metrics. The server processes these requests within the ERASER framework, calculating the inference latency and computation overhead.

- Average Waiting Time (AWT): The time difference between the submission of the inference request and the return of the prediction result is calculated, with the average waiting time representing the inference latency.
- Number of Retraining (NoR): The number of times each constituent model has been trained is counted and summed to represent the computation overhead.

6.2 Overview

To answer **RQ1**, we report the overall performance of eight different methods on four real-world datasets in Table 3. The numbers in parentheses indicate improvements over SISA (due to space limitations, AWT in the table retains only two decimal places, while the numbers in parentheses are calculated based on AWT before rounding). In the experiment, we fix the number of shards to 20 and the total number of requests to 5,000, of which 10% are unlearning requests. The submission time of all requests follows a uniform distribution within a time interval, and the length of the time interval is set to the number of unlearning requests multiplied by the time required to retrain a constituent model. For methods with a threshold of uncertification ratio, the threshold is set to 0.05.

Regarding inference latency, all methods show significant improvements over SISA, with DIMP achieving up to 1,290 times faster response than SISA. In terms of computation overhead, all methods consume less than SISA except DIMP, with STTP and DTTP consuming up to 69% less computing resources than SISA.

Different methods trade-off on various evaluation metrics, which is consistent with the analysis in Section 5.2.

6.3 Parameters Analysis

To answer **RQ2**, we use the control variable method to study the influence of various parameters on the performance of ERASER. Due to space limitations, we only show experimental results on Purchase and SVHN. To prevent some lines from being crowded together, we take the logarithm of AWT in the figures, so negative results may be seen when the original AWT is less than 1.

Number of Shards. We demonstrate the impact of the number of shards on AWT and NoR in Figure 4.

In general, as the number of shards increases, inference latency decreases. This is because given the same number of unlearning requests, having more constituent models reduces the proportion of models needing updates, thus increasing the probability of getting certified prediction results. However, when there are too many shards (e.g. more than 30), the

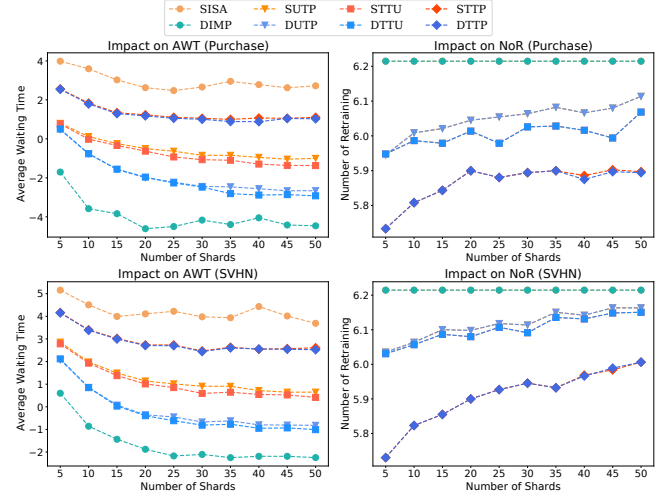


Figure 4: Evaluation on Number of Shards.

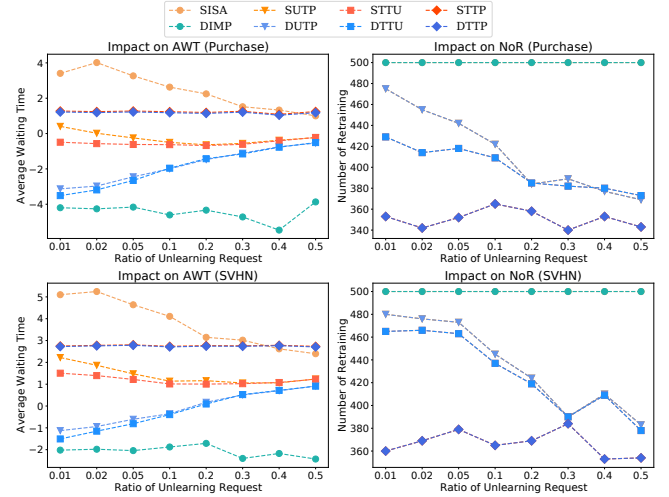


Figure 5: Evaluation on Ratio of Unlearning Requests.

decrease in AWT becomes less significant. This is attributed to the fact that each constituent model has lower accuracy, resulting in a higher number of uncertified prediction results.

The NoR of SISA and DIMP is fixed to the number of unlearning requests, as each unlearning request triggers an unlearning update. The NoR of other methods is positively correlated with the number of shards, because when there are numerous shards, the distribution of unlearning requests among constituent models becomes more dispersed, reducing the average number of unlearning requests executed during a single unlearning update. Note that although there are eight methods in total, it appears that only four lines are visible in the figure, as methods that differ solely in Option I overlap.

Ratio of Unlearning Requests. To investigate the impact

Table 3: Overview of Results on Four Datasets.

Dataset	Metric	SISA	DIMP	SUTP	DUTP	STTU	DTTU	STTP	DTTP
PURCHASE	AWT	14.73	0.01($\times 1290.73$)	0.57($\times 26.02$)	0.14($\times 105.64$)	0.46($\times 32.25$)	0.15($\times 99.41$)	3.31($\times 4.45$)	3.14($\times 4.70$)
	NoR	500	500($\times 1.000$)	412($\times 0.824$)	412($\times 0.824$)	399($\times 0.798$)	399($\times 0.798$)	350($\times 0.700$)	350($\times 0.700$)
SVHN	AWT	107.55	0.17($\times 647.44$)	3.40($\times 31.63$)	0.74($\times 145.22$)	2.78($\times 38.70$)	0.67($\times 159.82$)	16.40($\times 6.56$)	16.01($\times 6.72$)
	NoR	500	500($\times 1.000$)	429($\times 0.858$)	429($\times 0.858$)	421($\times 0.842$)	421($\times 0.842$)	345($\times 0.690$)	345($\times 0.690$)
MNIST	AWT	21.34	0.03($\times 801.63$)	0.63($\times 34.09$)	0.13($\times 159.86$)	0.54($\times 39.76$)	0.12($\times 181.95$)	3.04($\times 7.03$)	2.85($\times 7.49$)
	NoR	500	500($\times 1.000$)	447($\times 0.894$)	447($\times 0.894$)	434($\times 0.868$)	434($\times 0.868$)	377($\times 0.754$)	377($\times 0.754$)
IMAGENETTE	AWT	1387.59	14.76($\times 94.01$)	175.64($\times 7.90$)	45.24($\times 30.67$)	147.91($\times 9.38$)	39.95($\times 34.73$)	536.35($\times 2.59$)	521.77($\times 2.66$)
	NoR	500	500($\times 1.000$)	476($\times 0.952$)	476($\times 0.952$)	474($\times 0.948$)	474($\times 0.948$)	405($\times 0.810$)	405($\times 0.810$)

of the ratio of unlearning requests on ERASER’s performance, we fix the number of unlearning requests at 500 and adjust the ratio to determine the number of inference requests. The results are shown in Figure 5.

The computation overhead of SUTP and DUTP decreases as the ratio increases because a higher number of inference requests increases the likelihood of yielding at least one uncertified prediction result, leading to more frequent unlearning updates. However, the computation overhead of STTP and DTTP is almost unaffected by the ratio, as their unlearning update triggering condition depends on the proportion of uncertified requests in the total number of inference requests, which is not influenced by the absolute quantity.

The inference latency of SISA decreases with the decrease of inference requests, as too many inference requests prevent the server from fully utilizing its parallel capacity. For instance, if two unlearning requests arrive consecutively, the server can retrain their corresponding constituent models in parallel; however, if an inference request is inserted between two unlearning requests, the inference request must wait for the first unlearning request to be executed, and the second unlearning request has to wait for the processing of the inference request, making the execution of these two unlearning requests sequential. For methods such as SUTP and STTU that maintain a single context, more frequent unlearning updates lead to longer AWT. On the other hand, for DUTP and DTTU, which maintain both contexts, although the number of uncertified inferences increases with the total number of inference requests, the uncertification proportion decreases. In other words, the proportion of inference requests that need to wait decreases, resulting in a reduction in AWT. The inference latency of the remaining three methods is almost unaffected by the ratio of unlearning requests.

Request Density. In the experiments in Sect.6.2, we set the length of the time interval to the number of unlearning requests multiplied by the time required to retrain a constituent model. To explore the impact of request density on ERASER’s performance, we divide the basic time interval length by a coefficient; the larger the coefficient, the shorter the time interval, and the denser the arrival of requests. The effect of Request Density on ERASER is shown in Figure 6. The NoR

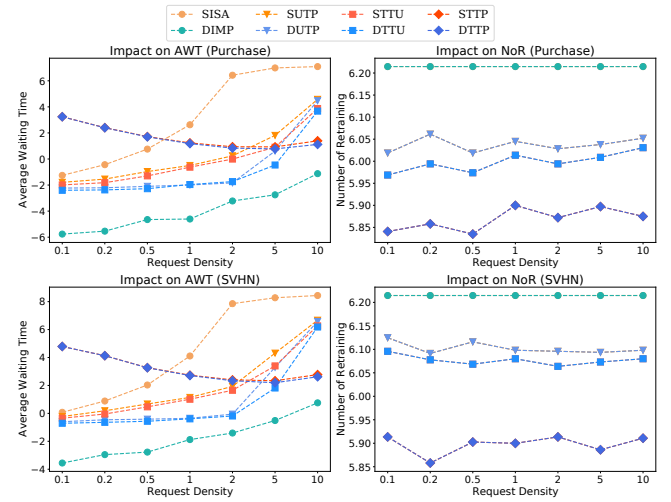


Figure 6: Evaluation on Request Density.

of all methods is not significantly related to density.

Except for STTP and DTTP, the AWT of all methods increases with increasing density because the probability that some constituent models are being updated when inference requests are submitted to the server becomes higher due to the shorter overall time interval. However, STTP and DTTP show the opposite trend, which is due to the composition of the waiting time. The waiting time of inference requests in these two methods primarily depends on waiting for the uncertification ratio to reach the threshold. Therefore, the higher the request density, the faster the uncertification ratio reaches the threshold, and thus the waiting time decreases.

Threshold of Uncertification Ratio. The threshold-triggered methods initiate an unlearning update once the uncertification threshold is exceeded. We show the impact of the threshold on the performance of these four methods in Figure 7. To save space, we plot AWT and NoR in the same figure.

The NoR and threshold of these four methods are negatively correlated because a higher threshold requires more uncertified predictions to trigger retraining. The inference latency of

Table 4: Impact of Request Distribution on Imagenette.

Metric	Distribution	SISA	DIMP	SUTP	DUTP	STTU	DTTU	STTP	DTTP
AWT	unimodal	7526.3	16.1($\times 467.6$)	207.1($\times 36.3$)	49.5($\times 152.0$)	175.7($\times 42.8$)	43.4($\times 173.3$)	557.8($\times 13.5$)	542.2($\times 13.9$)
	unimodal($\mu = \frac{T}{4}$)	21373.9	16.6($\times 1291.1$)	241.5($\times 88.5$)	54.7($\times 391.0$)	212.4($\times 100.7$)	50.0($\times 427.5$)	632.4($\times 33.8$)	609.4($\times 35.1$)
	unimodal($\mu = \frac{3T}{4}$)	16157.9	16.88($\times 957.3$)	256.6($\times 63.0$)	54.7($\times 295.2$)	226.9($\times 71.2$)	50.4($\times 320.9$)	443.4($\times 36.4$)	431.0($\times 37.5$)
	unimodal($\sigma = \frac{T}{2}$)	1715.2	14.73($\times 116.4$)	166.5($\times 10.3$)	44.5($\times 38.6$)	157.5($\times 10.9$)	42.5($\times 40.4$)	531.5($\times 3.2$)	514.7($\times 3.3$)
	unimodal($\sigma = \frac{T}{4}$)	22274.0	17.2($\times 1298.9$)	252.4($\times 88.3$)	56.6($\times 393.6$)	231.2($\times 96.0$)	54.6($\times 408.0$)	506.4($\times 44.0$)	489.4($\times 45.5$)
	bimodal	5522.1	14.2($\times 388.4$)	190.0($\times 29.01$)	46.8($\times 118.0$)	166.7($\times 33.12$)	42.8($\times 129.1$)	508.8($\times 10.9$)	492.2($\times 11.2$)
	trimodal	3649.7	15.8($\times 231.5$)	185.6($\times 19.7$)	47.0($\times 77.7$)	175.3($\times 20.8$)	44.4($\times 82.1$)	548.4($\times 6.7$)	530.7($\times 6.9$)
	quadmodal	1907.7	15.7($\times 121.3$)	180.0($\times 10.60$)	45.8($\times 41.6$)	168.7($\times 11.3$)	43.4($\times 44.1$)	559.4($\times 3.4$)	543.8($\times 3.5$)
	diff- μ ($\mu_u = \frac{T}{4}$, $\mu_l = \frac{3T}{4}$)	6754.8	10.9($\times 618.1$)	144.6($\times 46.7$)	36.87($\times 183.2$)	134.3($\times 50.3$)	35.9($\times 188.2$)	406.2($\times 16.6$)	387.6($\times 17.4$)
	diff- μ ($\mu_u = \frac{T}{4}$, $\mu_l = \frac{T}{4}$)	3144.5	12.0($\times 262.4$)	133.9($\times 23.5$)	36.8($\times 85.5$)	126.1($\times 24.9$)	34.9($\times 90.1$)	672.2($\times 4.7$)	660.0($\times 4.8$)
NoR	diff- σ ($\sigma_u = \frac{T}{2}$, $\sigma_l = \frac{T}{4}$)	2079.9	13.3($\times 156.7$)	164.0($\times 12.7$)	41.9($\times 49.6$)	147.7($\times 14.1$)	39.3($\times 52.9$)	553.9($\times 3.8$)	538.2($\times 3.9$)
	diff- σ ($\sigma_u = \frac{T}{4}$, $\sigma_l = \frac{T}{2}$)	14436.8	15.0($\times 961.9$)	213.6($\times 67.6$)	55.5($\times 260.3$)	188.5($\times 76.6$)	50.7($\times 284.7$)	517.2($\times 27.9$)	506.2($\times 28.5$)
	unimodal	500	500($\times 1.000$)	473($\times 0.946$)	473($\times 0.940$)	470($\times 0.940$)	401($\times 0.802$)	401($\times 0.802$)	
	unimodal($\mu = \frac{T}{4}$)	500	500($\times 1.000$)	480($\times 0.960$)	480($\times 0.954$)	477($\times 0.954$)	406($\times 0.812$)	406($\times 0.812$)	
	unimodal($\mu = \frac{3T}{4}$)	500	500($\times 1.000$)	475($\times 0.950$)	475($\times 0.950$)	473($\times 0.946$)	401($\times 0.802$)	401($\times 0.802$)	
	unimodal($\sigma = \frac{T}{4}$)	500	500($\times 1.000$)	478($\times 0.956$)	478($\times 0.956$)	478($\times 0.956$)	416($\times 0.832$)	416($\times 0.832$)	
	unimodal($\sigma = \frac{T}{2}$)	500	500($\times 1.000$)	465($\times 0.930$)	465($\times 0.930$)	463($\times 0.926$)	393($\times 0.786$)	393($\times 0.786$)	
	bimodal	500	500($\times 1.000$)	475($\times 0.950$)	475($\times 0.950$)	472($\times 0.944$)	402($\times 0.804$)	402($\times 0.804$)	
	trimodal	500	500($\times 1.000$)	479($\times 0.958$)	479($\times 0.958$)	476($\times 0.952$)	412($\times 0.824$)	412($\times 0.824$)	
	quadmodal	500	500($\times 1.000$)	482($\times 0.964$)	482($\times 0.964$)	480($\times 0.960$)	413($\times 0.826$)	413($\times 0.826$)	
diff- μ ($\mu_u = \frac{T}{4}$, $\mu_l = \frac{3T}{4}$)	500	500($\times 1.000$)	457($\times 0.914$)	457($\times 0.914$)	454($\times 0.908$)	454($\times 0.908$)	414($\times 0.828$)	414($\times 0.828$)	
	diff- μ ($\mu_u = \frac{T}{4}$, $\mu_l = \frac{T}{4}$)	500	500($\times 1.000$)	464($\times 0.928$)	464($\times 0.928$)	461($\times 0.922$)	461($\times 0.922$)	319($\times 0.638$)	319($\times 0.638$)
	diff- σ ($\sigma_u = \frac{T}{2}$, $\sigma_l = \frac{T}{4}$)	500	500($\times 1.000$)	478($\times 0.956$)	478($\times 0.956$)	475($\times 0.950$)	412($\times 0.824$)	412($\times 0.824$)	
	diff- σ ($\sigma_u = \frac{T}{4}$, $\sigma_l = \frac{T}{2}$)	500	500($\times 1.000$)	474($\times 0.948$)	474($\times 0.948$)	467($\times 0.934$)	401($\times 0.802$)	401($\times 0.802$)	

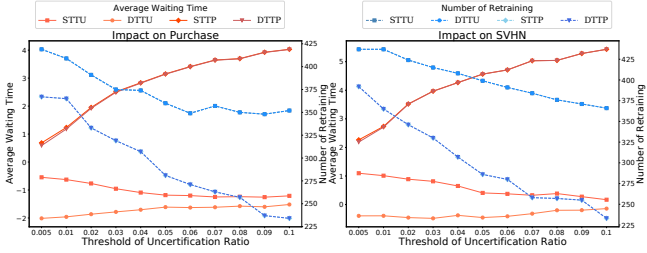


Figure 7: Evaluation on Threshold of Uncertification Ratio.

STTP and DTTP increases with an increasing threshold, as inference requests in the uncertification list must first wait for the ratio to reach the threshold, and a larger threshold results in a longer waiting time. The AWT of STTU decreases with an increasing threshold, because a higher threshold reduces NoR, and the number of inference requests that need to wait for the completion of unlearning updates also decreases. The AWT of DTTU remains almost unchanged with the increasing threshold, possibly because the server can still respond to inference requests during unlearning updates.

6.4 Temporal Distribution of Requests

In previous experiments, we assume that all requests are uniformly distributed over time and that both types of requests share the same distribution. However, this may not be the case

in real-world scenarios. We use the Gaussian distribution as an example to study the effects of the temporal distribution of requests on the performance of ERASER to answer **RQ3**. We focus on three distribution characteristics: 1. The mean and variance; 2. Unimodal or multimodal; 3. Differences between unlearning and inference request distributions. Assuming the time interval is $[0, T]$, if the sampled arrival time lies outside the interval, we will re-sample. Experimental results on the Imagenette dataset are shown in Table 4.

Initially, we assume that both unlearning and inference requests follow a Gaussian distribution with a mean of $\mu = \frac{T}{2}$ and a standard deviation of $\sigma = \frac{T}{3}$. The first row of the table displays the results. The inference latency increases compared to the uniform distribution in Table 3, while the NoR slightly decreases. We then alter the mean to $\mu = \frac{T}{4}$ and $\mu = \frac{3T}{4}$, corresponding to rows 2-3. The inference latency increases further, potentially due to the resampling strategy. When the distribution's center is close to the interval's edge, resampling points outside the interval causes the peak to be higher. Next, we change the standard deviation to $\sigma = \frac{T}{2}$ and $\sigma = \frac{T}{4}$, corresponding to rows 4-5. A larger standard deviation flattens the distribution.

Considering that the temporal distribution of requests may have multiple peaks, we assume several multimodal Gaussian distributions, corresponding to rows 6-8. The results show that as the number of peaks increases, the inference latency decreases and the computation overhead increases, because a distribution with more peaks resembles a uniform distribution

more closely.

Lastly, we examine cases where unlearning and inference request distributions differ. We first consider different mean values (rows 9-10). Regardless of whether the unlearning or inference request distribution peak came first, both inference latency and computation overhead decreases, sometimes even surpassing uniform distribution performance. This is because inference requests are more likely to wait while numerous unlearning requests are submitted concurrently. Staggering the peaks of the two distributions results in fewer waiting inference requests and reduces unlearning update frequency, enabling single unlearning updates to process more requests. However, when the inference request distribution peak comes first, i.e., $\mu_u = \frac{3T}{4}$ and $\mu_i = \frac{T}{4}$, the inference latency for STTP and DTTP becomes significantly high. This is because some inference requests' prediction results may be uncertified at the peak, but the ratio might not reach the threshold, forcing them to wait until the unlearning request peak for reprocessing. We also consider different standard deviations (rows 11-12). Higher concentration of unlearning requests leads to increased inference latency, while the impact of higher concentration of inference requests is relatively small.

Please refer to Appendix F for more results.

7 Conclusion and Future Work

In this paper, we reveal that handling unlearning requests in an inference-oblivious under MLaaS setting can introduce two new security and privacy vulnerabilities. We proposed a pioneering framework, ERASER, for inference serving-aware machine unlearning that simultaneously serves both inference requests from queriers and unlearning requests from data owners. ERASER devised a novel certified inference consistency approach to reduce inference latency without introducing extra privacy risks for unlearning requested data. It also offers three groups of design options, providing seven specific variants tailored to different MLaaS environments and design objectives. Our extensive empirical results demonstrate the effectiveness of ERASER across various settings.

Future work includes 1) Studying more optimal design choices (e.g., better unlearning timing) that can adapt to the workloads of inference and unlearning requests; 2) Considering other critical factors (e.g., resources provision and cost) in terms of their security and privacy implications, as well as how to achieve better Pareto frontiers among all factors.

References

- [1] Amazon sagemaker. <https://aws.amazon.com/sagemaker>, 2018.
- [2] Amazon web services. <https://aws.amazon.com/>, 2018.
- [3] Google cloud. <https://cloud.google.com/>, 2018.
- [4] Microsoft azure cloud computing platform and services. <https://azure.microsoft.com/en-us/>, 2018.
- [5] Tensorflow serving for model deployment in production. <https://www.tensorflow.org/serving/>, 2018.
- [6] Nvidia triton inference server. <https://github.com/triton-inference-server/server>, 2020.
- [7] Marian Stewart Bartlett, Gwen Littlewort, Mark Frank, Claudia Lainscsek, Ian Fasel, and Javier Movellan. Recognizing facial expression: machine learning and application to spontaneous behavior. In *2005 IEEE Computer Society Conference on Computer Vision and Pattern Recognition (CVPR'05)*, volume 2, pages 568–573. IEEE, 2005.
- [8] John P. Beardwood. The new canadian consumer privacy protection act: A compliance briefing for privacy officers — a brief overview. *Computer Law Review International*, 22, 2021.
- [9] Lucas Bourtoule, Varun Chandrasekaran, Christopher A Choquette-Choo, Hengrui Jia, Adelin Travers, Baiwu Zhang, David Lie, and Nicolas Papernot. Machine unlearning. In *2021 IEEE Symposium on Security and Privacy (SP)*, pages 141–159. IEEE, 2021.
- [10] Jonathan Brophy and Daniel Lowd. Machine unlearning for random forests. In *International Conference on Machine Learning*, pages 1092–1104. PMLR, 2021.
- [11] Yinzhi Cao and Junfeng Yang. Towards making systems forget with machine unlearning. In *2015 IEEE symposium on security and privacy*, pages 463–480. IEEE, 2015.
- [12] Chong Chen, Fei Sun, Min Zhang, and Bolin Ding. Recommendation unlearning. In *Proceedings of the ACM Web Conference 2022*, pages 2768–2777, 2022.
- [13] Min Chen, Zhikun Zhang, Tianhao Wang, Michael Backes, Mathias Humbert, and Yang Zhang. When machine unlearning jeopardizes privacy. In *Proceedings of the 2021 ACM SIGSAC Conference on Computer and Communications Security*, pages 896–911, 2021.
- [14] Min Chen, Zhikun Zhang, Tianhao Wang, Michael Backes, Mathias Humbert, and Yang Zhang. Graph unlearning. In *Proceedings of the 2022 ACM SIGSAC Conference on Computer and Communications Security*, pages 499–513, 2022.
- [15] Daniel Crankshaw, Xin Wang, Giulio Zhou, Michael J. Franklin, Joseph E. Gonzalez, and Ion Stoica. Clipper: A low-latency online prediction serving system. In

Aditya Akella and Jon Howell, editors, *14th USENIX Symposium on Networked Systems Design and Implementation, NSDI 2017, Boston, MA, USA, March 27-29, 2017*, pages 613–627. USENIX Association, 2017.

[16] Weihao Cui, Han Zhao, Quan Chen, Hao Wei, Zirui Li, Deze Zeng, Chao Li, and Minyi Guo. Dvabatch: Diversity-aware multi-entry multi-exit batching for efficient processing of DNN services on gpus. In Jiri Schindler and Noa Zilberman, editors, *2022 USENIX Annual Technical Conference, USENIX ATC 2022, Carlsbad, CA, USA, July 11-13, 2022*, pages 183–198. USENIX Association, 2022.

[17] Weihao Cui, Han Zhao, Quan Chen, Ningxin Zheng, Jingwen Leng, Jieru Zhao, Zhuo Song, Tao Ma, Yong Yang, Chao Li, and Minyi Guo. Enable simultaneous DNN services based on deterministic operator overlap and precise latency prediction. In Bronis R. de Supinski, Mary W. Hall, and Todd Gamblin, editors, *International Conference for High Performance Computing, Networking, Storage and Analysis, SC 2021, St. Louis, Missouri, USA, November 14-19, 2021*, page 15. ACM, 2021.

[18] Jimmy Z Di, Jack Douglas, Jayadev Acharya, Gautam Kamath, and Ayush Sekhari. Hidden poison: Machine unlearning enables camouflaged poisoning attacks. In *NeurIPS ML Safety Workshop*, 2022.

[19] Antonio Ginart, Melody Guan, Gregory Valiant, and James Y Zou. Making ai forget you: Data deletion in machine learning. *Advances in neural information processing systems*, 32, 2019.

[20] Aditya Golatkar, Alessandro Achille, Avinash Ravichandran, Marzia Polito, and Stefano Soatto. Mixed-privacy forgetting in deep networks. In *Proceedings of the IEEE/CVF Conference on Computer Vision and Pattern Recognition*, pages 792–801, 2021.

[21] Aditya Golatkar, Alessandro Achille, and Stefano Soatto. Eternal sunshine of the spotless net: Selective forgetting in deep networks. In *Proceedings of the IEEE/CVF Conference on Computer Vision and Pattern Recognition*, pages 9304–9312, 2020.

[22] Aditya Golatkar, Alessandro Achille, and Stefano Soatto. Forgetting outside the box: Scrubbing deep networks of information accessible from input-output observations. In *Computer Vision–ECCV 2020: 16th European Conference, Glasgow, UK, August 23–28, 2020, Proceedings, Part XXIX 16*, pages 383–398. Springer, 2020.

[23] Laura Graves, Vineel Nagisetty, and Vijay Ganesh. Amnesiac machine learning. In *Proceedings of the AAAI Conference on Artificial Intelligence*, volume 35, pages 11516–11524, 2021.

[24] Arpan Gujarati, Reza Karimi, Safya Alzayat, Wei Hao, Antoine Kaufmann, Ymir Vigfusson, and Jonathan Mace. Serving dnns like clockwork: Performance predictability from the bottom up. In *14th USENIX Symposium on Operating Systems Design and Implementation, OSDI 2020, Virtual Event, November 4-6, 2020*, pages 443–462. USENIX Association, 2020.

[25] Jashwant Raj Gunasekaran, Cyan Subhra Mishra, Prashanth Thinakaran, Bikash Sharma, Mahmut Taylan Kandemir, and Chita R. Das. Cocktail: A multidimensional optimization for model serving in cloud. In *19th USENIX Symposium on Networked Systems Design and Implementation (NSDI 22)*, pages 1041–1057, Renton, WA, 2022.

[26] Chuan Guo, Tom Goldstein, Awni Hannun, and Laurens Van Der Maaten. Certified data removal from machine learning models. *arXiv preprint arXiv:1911.03030*, 2019.

[27] Udit Gupta, Samuel Hsia, Vikram Saraph, Xiaodong Wang, Brandon Reagen, Gu-Yeon Wei, Hsien-Hsin S Lee, David Brooks, and Carole-Jean Wu. Deeprecsys: A system for optimizing end-to-end at-scale neural recommendation inference. In *2020 ACM/IEEE 47th Annual International Symposium on Computer Architecture (ISCA)*, pages 982–995. IEEE, 2020.

[28] Johann Hauswald, Michael A Laurenzano, Yunqi Zhang, Cheng Li, Austin Rovinski, Arjun Khurana, Ronald G Dreslinski, Trevor Mudge, Vinicius Petrucci, Lingjia Tang, et al. Sirius: An open end-to-end voice and vision personal assistant and its implications for future warehouse scale computers. In *Proceedings of the Twentieth International Conference on Architectural Support for Programming Languages and Operating Systems*, pages 223–238, 2015.

[29] Kim Hazelwood, Sarah Bird, David Brooks, Soumith Chintala, Utku Diril, Dmytro Dzhulgakov, Mohamed Fawzy, Bill Jia, Yangqing Jia, Aditya Kalro, et al. Applied machine learning at facebook: A datacenter infrastructure perspective. In *2018 IEEE International Symposium on High Performance Computer Architecture (HPCA)*, pages 620–629. IEEE, 2018.

[30] Jeremy Howard. Imagenette dataset. <https://github.com/fastai/imagenette>, 2019.

[31] Hongsheng Hu, Shuo Wang, Jiamin Chang, Haonan Zhong, Ruoxi Sun, Shuang Hao, Haojin Zhu, and Min-hui Xue. A duty to forget, a right to be assured? exposing vulnerabilities in machine unlearning services. *CoRR*, abs/2309.08230, 2023.

[32] Hai Huang, Zhikun Zhang, Yun Shen, Michael Backes, Qi Li, and Yang Zhang. On the privacy risks of cell-based nas architectures. In *Proceedings of the 2022 ACM SIGSAC Conference on Computer and Communications Security*, pages 1427–1441, 2022.

[33] Zachary Izzo, Mary Anne Smart, Kamalika Chaudhuri, and James Zou. Approximate data deletion from machine learning models. In *International Conference on Artificial Intelligence and Statistics*, pages 2008–2016. PMLR, 2021.

[34] Jinyuan Jia, Xiaoyu Cao, and Neil Zhenqiang Gong. Intrinsic certified robustness of bagging against data poisoning attacks. In *Proceedings of the AAAI Conference on Artificial Intelligence*, volume 35, pages 7961–7969, 2021.

[35] Korbinian Koch and Marcus Soll. No matter how you slice it: Machine unlearning with sisa comes at the expense of minority classes. In *2023 IEEE Conference on Secure and Trustworthy Machine Learning (SatML)*, pages 622–637. IEEE, 2023.

[36] Yann LeCun, Léon Bottou, Yoshua Bengio, and Patrick Haffner. Gradient-based learning applied to document recognition. *Proc. IEEE*, 86(11):2278–2324, 1998.

[37] Alexander Levine and Soheil Feizi. Deep partition aggregation: Provable defenses against general poisoning attacks. In *9th International Conference on Learning Representations, ICLR 2021, Virtual Event, Austria, May 3-7, 2021*. OpenReview.net, 2021.

[38] Zheng Li and Yang Zhang. Membership leakage in label-only exposures. In *Proceedings of the 2021 ACM SIGSAC Conference on Computer and Communications Security*, pages 880–895, 2021.

[39] Yugeng Liu, Rui Wen, Xinlei He, Ahmed Salem, Zhikun Zhang, Michael Backes, Emiliano De Cristofaro, Mario Fritz, and Yang Zhang. {ML-Doctor}: Holistic risk assessment of inference attacks against machine learning models. In *31st USENIX Security Symposium (USENIX Security 22)*, pages 4525–4542, 2022.

[40] Ananth Mahadevan and Michael Mathioudakis. Certifiable machine unlearning for linear models. *arXiv preprint arXiv:2106.15093*, 2021.

[41] Alessandro Mantelero. The eu proposal for a general data protection regulation and the roots of the ‘right to be forgotten’. *Computer Law & Security Review*, 29(3):229–235, 2013.

[42] Neil G Marchant, Benjamin IP Rubinstein, and Scott Alfeld. Hard to forget: Poisoning attacks on certified machine unlearning. In *Proceedings of the AAAI Conference on Artificial Intelligence*, volume 36, pages 7691–7700, 2022.

[43] Ronak Mehta, Sourav Pal, Vikas Singh, and Sathya N Ravi. Deep unlearning via randomized conditionally independent hessians. In *Proceedings of the IEEE/CVF Conference on Computer Vision and Pattern Recognition*, pages 10422–10431, 2022.

[44] Seth Neel, Aaron Roth, and Saeed Sharifi-Malvajerdi. Descent-to-delete: Gradient-based methods for machine unlearning. In *Algorithmic Learning Theory*, pages 931–962. PMLR, 2021.

[45] Yuval Netzer, Tao Wang, Adam Coates, Alessandro Bissacco, Bo Wu, and Andrew Y. Ng. Reading digits in natural images with unsupervised feature learning. In *NIPS Workshop on Deep Learning and Unsupervised Feature Learning 2011*, 2011.

[46] Quoc Phong Nguyen, Bryan Kian Hsiang Low, and Patrick Jaillet. Variational bayesian unlearning. *Advances in Neural Information Processing Systems*, 33:16025–16036, 2020.

[47] State of California Office of the Attorney General. California consumer privacy act (ccpa). <https://oag.ca.gov/privacy/ccpa>, 2023.

[48] Alexandra Peste, Dan Alistarh, and Christoph H Lampert. Ssse: Efficiently erasing samples from trained machine learning models. *arXiv preprint arXiv:2107.03860*, 2021.

[49] Francisco Romero, Qian Li, Neeraja J. Yadwadkar, and Christos Kozyrakis. Infaas: Automated model-less inference serving. In Irina Calciu and Geoff Kuenning, editors, *2021 USENIX Annual Technical Conference, USENIX ATC 2021, July 14-16, 2021*, pages 397–411. USENIX Association, 2021.

[50] Cemal Okan Sakar, Suleyman Olcay Polat, Mete Katircioglu, and Yomi Castro. Real-time prediction of online shoppers’ purchasing intention using multilayer perceptron and LSTM recurrent neural networks. *Neural Comput. Appl.*, 31(10):6893–6908, 2019.

[51] Ahmed Salem, Yang Zhang, Mathias Humbert, Pascal Berrang, Mario Fritz, and Michael Backes. MI-leaks: Model and data independent membership inference attacks and defenses on machine learning models. In *26th Annual Network and Distributed System Security Symposium, NDSS 2019, San Diego, California, USA, February 24-27, 2019*. The Internet Society, 2019.

[52] Sebastian Schelter, Stefan Grafberger, and Ted Dunning. Hedgecut: Maintaining randomised trees for low-latency machine unlearning. In *Proceedings of the 2021 International Conference on Management of Data*, pages 1545–1557, 2021.

[53] Ayush Sekhari, Jayadev Acharya, Gautam Kamath, and Ananda Theertha Suresh. Remember what you want to forget: Algorithms for machine unlearning. *Advances in Neural Information Processing Systems*, 34:18075–18086, 2021.

[54] Steven A Shaya, Neal Matheson, John Anthony Singarayar, Nikiforos Kollias, and Jeffrey Adam Bloom. Intelligent performance-based product recommendation system, October 5 2010. US Patent 7,809,601.

[55] Reza Shokri, Marco Stronati, Congzheng Song, and Vitaly Shmatikov. Membership inference attacks against machine learning models. In *2017 IEEE symposium on security and privacy (SP)*, pages 3–18. IEEE, 2017.

[56] Enayat Ullah, Tung Mai, Anup Rao, Ryan A Rossi, and Raman Arora. Machine unlearning via algorithmic stability. In *Conference on Learning Theory*, pages 4126–4142. PMLR, 2021.

[57] Wenxiao Wang, Alexander J Levine, and Soheil Feizi. Improved certified defenses against data poisoning with (deterministic) finite aggregation. In *International Conference on Machine Learning*, pages 22769–22783. PMLR, 2022.

[58] Alexander Warnecke, Lukas Pirch, Christian Wressneger, and Konrad Rieck. Machine unlearning of features and labels. *arXiv preprint arXiv:2108.11577*, 2021.

[59] Alexander Warnecke, Lukas Pirch, Christian Wressneger, and Konrad Rieck. Machine unlearning of features and labels. In *30th Annual Network and Distributed System Security Symposium, NDSS 2023, San Diego, California, USA, February 27 - March 3, 2023*. The Internet Society, 2023.

[60] Yinjun Wu, Edgar Dobriban, and Susan Davidson. Deltagrad: Rapid retraining of machine learning models. In *International Conference on Machine Learning*, pages 10355–10366. PMLR, 2020.

[61] Haonan Yan, Xiaoguang Li, Ziyao Guo, Hui Li, Fenghua Li, and Xiaodong Lin. Arcane: An efficient architecture for exact machine unlearning. In *Proceedings of the Thirty-First International Joint Conference on Artificial Intelligence, IJCAI-22*, pages 4006–4013, 2022.

[62] Chengliang Zhang, Minchen Yu, Wei Wang, and Feng Yan. Mark: Exploiting cloud services for cost-effective, slo-aware machine learning inference serving. In *Dahlia* Malkhi and Dan Tsafrir, editors, *2019 USENIX Annual Technical Conference, USENIX ATC 2019, Renton, WA, USA, July 10-12, 2019*, pages 1049–1062. USENIX Association, 2019.

[63] Zijie Zhang, Yang Zhou, Xin Zhao, Tianshi Che, and Lingjuan Lyu. Prompt certified machine unlearning with randomized gradient smoothing and quantization. *Advances in Neural Information Processing Systems*, 35:13433–13455, 2022.

Appendices

In the following, Appendix A clarifies the research goal of this paper; Appendix B contains more theoretical results; Appendix C-D provides more content about algorithm design; Appendix E discuss potential malicious request and how to mitigate; Appendix F presents more experiment results.

A What we do not achieve in this paper

We briefly discuss what we do not aim to achieve in this paper. *Regarding extra privacy risk:* We focus on ensuring that data owners who have submitted unlearning requests do not suffer from extra privacy risk due to the postponed unlearning execution. However, we do not address other sources of privacy threats, such as general privacy attacks considered in MIA literature where any data owners can be the victim [38, 39, 51, 55], or the MIA considered in [13] that discerns the difference between model predictions before and after machine unlearning. We also do not address the issue of attackers impersonating data owners to submit fraudulent unlearning requests, as we consider this to fall under the domain of user authentication, which is orthogonal to the research objectives of this paper.

Regarding extra inference latency: We focus on reducing the extra inference latency caused by unlearning requests. However, we do not address other sources of inference latency in the original inference serving pipeline that can be raised from various external factors (e.g., network issues, busty workload) or internal factors (availability of hardware resources (GPUs, memories) changes, concurrency from other processes). In addition, we do not seek to accelerate the machine unlearning mechanism itself, as this has been studied in many existing literature and is not the focus of this paper.

B Additional Theoretical Results

B.1 Deferred proof of Theorem 1

Proof. According to the pending unlearning requests, We have the following two cases:

Case I. $S_k^t = S_k^0$: There is no pending unlearning requests to Shard k , which implies $f_k^t(\mathbf{z}) = f_k^0(\mathbf{z})$ upon step t ;

Case II. $\mathcal{S}_k^t \neq \mathcal{S}_k^0$: there is one or multiple pending unlearning requests to Shard k upon timestamp t , which has the potential of $f_k^t(\mathbf{z}) \neq f_k^0(\mathbf{z})$.

According to the prediction results, Case II can be further divided into three subcases. The aim is to estimate whether the largest possible $\text{Count}_{y_b}^t(\mathbf{z})$ will be greater than the smallest possible $\text{Count}_{y_a}^t(\mathbf{z})$, which is the most likely situation (i.e., the easiest case for inference inconsistency) to flip the final prediction result from y_a to y_b and the inference consistency no longer holds. For any $\{k \in [K] | \mathcal{S}_k^t \neq \mathcal{S}_k^0\}$, we have three possible prediction results for $f_k^0(\mathbf{z})$ and the potential $f_k^t(\mathbf{z})$:

1. if $f_k^0(\mathbf{z}) = y_a$, and the potential $f_k^t(\mathbf{z}) = y_b$;
2. if $f_k^0(\mathbf{z}) = y_b$, and the potential $f_k^t(\mathbf{z}) = y_b$;
3. $f_k^0(\mathbf{z}) \neq y_a \& f_k^0(\mathbf{z}) \neq y_b$, and the potential $f_k^t(\mathbf{z}) = y_b$.

The counts of the above three subcases correspond exactly to $\gamma_1, \gamma_2, \gamma_3$, which can be collected based solely on the prediction results from $f_1^0(\mathbf{z}), \dots, f_K^0(\mathbf{z})$. Then, we have the lower bound of $\text{Count}_{y_a}^t(\mathbf{x})$ to be

$$\text{Count}_{y_a}^t(\mathbf{z}) \leq \text{Count}_{y_a}^0(\mathbf{z}) - \gamma_1, \quad (12)$$

and the upper bound of $\text{Count}_{y_b}^t(\mathbf{z})$ to be

$$\text{Count}_{y_b}^t(\mathbf{z}) \geq \text{Count}_{y_b}^0(\mathbf{z}) + \gamma_1 + \gamma_3. \quad (13)$$

As a result, as long as for all $y_b \neq y_a$, $\text{Count}_{y_a}^0(\mathbf{z}) - \gamma_1 > \text{Count}_{y_b}^0(\mathbf{z}) + \gamma_1 + \gamma_3$, which can be relaxed to $2\gamma_1 + \gamma_3 \leq \text{Count}_{y_a}^0(\mathbf{z}) - \text{Count}_{y_b}^0(\mathbf{z}) - \mathbb{1}(y < y_a) = \Gamma$, we have $F^t(\mathbf{z}) = F^0(\mathbf{z})$. \square

B.2 Straightforward adaptation from [37]

Theorem 4. (*Straightforward adaptation from [37]*) Under the same setting with Theorem 1, let the number of impacted shards be γ as defined below,

$$\gamma := |\{k \in [K] | \mathcal{S}_k^t \neq \mathcal{S}_k^0\}|. \quad (14)$$

The model can respond to the inference request of \mathbf{x} without retraining, while ensuring the prediction is exactly the same as the otherwise retrained prediction, i.e., $F^t(\mathbf{z}) = F^0(\mathbf{z}) = y_a$, as long as the following condition holds: $\forall y \neq y_a$,

$$2\gamma \leq \Gamma, \quad (15)$$

where $\Gamma = \max_{\forall y \neq y_a} \{\text{Count}_{y_a}^0(\mathbf{z}) - \text{Count}_y^0(\mathbf{z}) - \mathbb{1}(y < y_a)\}$.

Proof. (*Straightforward adaptation from [37]*) Our aim is to prove that, as long as $\gamma \leq \Gamma$, we certify that $F^t(\mathbf{z}) = F^0(\mathbf{z})$, i.e., the original model will provide exactly the same prediction label with the otherwise retrained model. Consequently, it allows for serving the inference request on \mathbf{z} without executing the actual data forgotten requests of U^t by retraining

the model. There are two cases: 1) $\mathcal{S}_k^t = \mathcal{S}_k^0$, there is no data deletion in Shard k , which implies $f_k^t(\mathbf{z}) = f_k^0(\mathbf{z})$ upon step t ; 2) $\mathcal{S}_k^t \neq \mathcal{S}_k^0$, there is one or multiple data deletions in Shard k upon step t , which can lead to $f_k^t(\mathbf{z}) \neq f_k^0(\mathbf{z})$. Thus, by Case 2, there are at most τ constituent classifiers that can have $f_k^t(\mathbf{z}) \neq f_k^0(\mathbf{z})$. For any $y \in \mathbb{Y}$, we have

$$|\text{Count}_y^0(\mathbf{x}) - \text{Count}_y^t(\mathbf{x})| \leq \gamma. \quad (16)$$

Let $y_a = F^0(\mathbf{z})$. As long as the following condition holds

$$\text{Count}_{y_a}^t(\mathbf{z}) > \text{Count}_y^t(\mathbf{z}), \text{ if } y < y_a \quad (17)$$

$$\text{Count}_{y_a}^t(\mathbf{z}) \geq \text{Count}_y^t(\mathbf{z}), \text{ if } y > y_a, \quad (18)$$

which can be equivalently described by

$$\forall y \neq y_a, \text{Count}_{y_a}^t(\mathbf{x}) \geq \text{Count}_y^t(\mathbf{x}) + \mathbb{1}(y < y_a), \quad (19)$$

we will have $F^t(\mathbf{z}) = y_a$. As a result, we have $F^t(\mathbf{z}) = y_a$ if

$$\text{Count}_{y_a}^t(\mathbf{z}) \geq \text{Count}_{y_a}^0(\mathbf{z}) - \gamma \quad (20)$$

$$\text{Count}_y^0(\mathbf{z}) + \gamma \geq \text{Count}_y^t(\mathbf{z}) \quad (21)$$

In order to have eq.(19), it suffices to ensure

$$\text{Count}_{y_a}^0(\mathbf{z}) - \gamma \geq \text{Count}_y^0(\mathbf{z}) + \gamma + \mathbb{1}(y < y_a). \quad (22)$$

As a result, as long as $\gamma \leq \Gamma$ with $\Gamma = \frac{1}{2}(\text{Count}_{y_a}^0(\mathbf{x}) - \text{Count}_y^0(\mathbf{x}) - \mathbb{1}(y < y_a))$, we have $F^t(\mathbf{z}) = F^0(\mathbf{z})$. \square

Since $\gamma = \gamma_1 + \gamma_2 + \gamma_3$, it is obvious that $2\gamma \geq 2\gamma_1 + \gamma_3$. Thus, it indicates that Theorem 1 provides a more fine-grained certification bound than Theorem 4, which also shows that our certification analysis is tailored to machine unlearning in MLaaS.

B.3 Deferred proof of Theorem 2

Assume the time required to retrain a constituent model is fixed at r , the number of unlearning requests is n_u , the number of inference requests is n_i , the arrival time interval for all requests is $[0, T]$. For simplicity, we assume that all unlearning requests arrive at fixed time intervals, with an unlearning request arriving every $\frac{T}{n_u}$ starting from $t = 0$. Since the time taken for a single inference is almost negligible compared to unlearning, the waiting time for inference requests mainly depends on the duration of unlearning. As such, we do not consider the time taken for inference when calculating waiting time.

Proof. For a certain inference request, let its arrival time at the server be t_i . Assume it is between the arrival time of the i -th unlearning request and the $(i+1)$ -th unlearning request, i.e., $t_i \in [(i-1) \cdot \frac{T}{n_u}, i \cdot \frac{T}{n_u}]$. The retraining time for the i -th unlearning request is $[(i-1) \cdot \frac{T}{n_u}, (i-1) \cdot \frac{T}{n_u} + r]$.

Based on whether the time required to train a constituent model, r , is greater than the arrival interval of unlearning requests, $\frac{T}{n_u}$, we have two cases:

1. $r \leq \frac{T}{n_u}$. In this case, the waiting time for the prediction, w_{sisa} , can be expressed as:

$$w_{sisa} = \begin{cases} (i-1) \cdot \frac{T}{n_u} + r - t_i, & t_i \in [(i-1) \cdot \frac{T}{n_u}, (i-1) \cdot \frac{T}{n_u} + r] \\ 0, & t_i \in [(i-1) \cdot \frac{T}{n_u} + r, i \cdot \frac{T}{n_u}]. \end{cases} \quad (23)$$

Since t_i follows a uniform distribution, i.e.,

$$P(t_i) = \frac{n_u}{T}, \quad t_i \in [(i-1) \cdot \frac{T}{n_u}, i \cdot \frac{T}{n_u}] \quad (24)$$

Therefore, the expected value of w_{sisa} is:

$$\mathbb{E}(w_{sisa}) = \int_{(i-1) \cdot \frac{T}{n_u}}^{(i-1) \cdot \frac{T}{n_u} + r} \frac{n_u}{T} ((i-1) \cdot \frac{T}{n_u} + r - t_i) dt_i \quad (25)$$

$$= \frac{n_u r^2}{2T}. \quad (26)$$

2. $r > \frac{T}{n_u}$. In this case, the waiting time for the prediction, w_{sisa} , can be expressed as:

$$w_{sisa} = (i-1) \cdot \frac{T}{n_u} + r - t_i. \quad (27)$$

The expected value of w_{sisa} is

$$\mathbb{E}(w_{sisa}) = \int_{(i-1) \cdot \frac{T}{n_u}}^{i \cdot \frac{T}{n_u}} \frac{n_u}{T} ((i-1) \cdot \frac{T}{n_u} + r - t_i) dt_i \quad (28)$$

$$= r - \frac{T}{2n_u}. \quad (29)$$

To conclude, we have proved that

$$\mathbb{E}(w_{sisa}) = \begin{cases} \frac{n_u r^2}{2T}, & r \leq \frac{T}{n_u} \\ r - \frac{T}{2n_u}, & r > \frac{T}{n_u}. \end{cases} \quad (30)$$

□

B.4 Deferred proof of Theorem 3

Proof. The number of constituent models being retrained, k_r , when an inference request arrives can be represented as:

$$k_r = \begin{cases} \lfloor \frac{rn_u}{T} \rfloor, & (t_i \bmod \frac{T}{n_u}) > r \bmod (\frac{T}{n_u}) \\ \lfloor \frac{rn_u}{T} \rfloor + 1, & (t_i \bmod \frac{T}{n_u}) \leq (r \bmod \frac{T}{n_u}). \end{cases} \quad (31)$$

The time difference, t_d , between the arrival of the inference request and the nearest completion of retraining can be represented as:

$$t_d = \begin{cases} \frac{T}{n_u} + (r \bmod \frac{T}{n_u}) - (t_i \bmod \frac{T}{n_u}), & (t_i \bmod \frac{T}{n_u}) > (r \bmod \frac{T}{n_u}) \\ (r \bmod \frac{T}{n_u}) - (t_i \bmod \frac{T}{n_u}), & (t_i \bmod \frac{T}{n_u}) \leq (r \bmod \frac{T}{n_u}). \end{cases} \quad (32)$$

For each inference request, a maximum of k_r certification judgements will occur, which are when the inference request arrives and when each constituent model finishes retraining (excluding the last finished constituent model, because when all retraining constituent models are completed, the prediction result must be certified).

Therefore, the expected waiting time, w_{dimp} , for the prediction can be represented as:

$$\mathbb{E}(w_{dimp}) = \sum_{i=1}^{k-1} ((1 - p_{uc}) p_{uc}^i \cdot (t_d + \frac{(i-1)T}{n_u})) \quad (33)$$

$$+ p_{uc}^k (t_d + \frac{(k-1)T}{n_u}) + (1 - p_{uc}) \cdot 0 \quad (34)$$

$$= p_{uc} \cdot t_d + \sum_{i=2}^{k-1} ((1 - p_{uc}) p_{uc}^i \cdot \frac{(i-1)T}{n_u}) \quad (35)$$

$$+ p_{uc}^k \frac{(k-1)T}{n_u} \quad (36)$$

This expression can hardly be simplified into a more intuitive form, but we can find a relatively concise upper bound for the expression: if the prediction result is uncertified when the inference request arrives, we skip all subsequent certification judgments and wait for all the retraining constituent models to complete their retraining before returning the prediction result. Obviously, this would result in a strictly longer waiting time, which is the same as the waiting time of SISA. Therefore, we can derive that:

$$\mathbb{E}(w_{dimp}) \leq (1 - p_{uc}) \cdot 0 + p_{uc} \cdot \mathbb{E}(w_{sisa}) \quad (37)$$

$$= \begin{cases} p_{uc} \cdot \frac{n_u r^2}{2T}, & r \leq \frac{T}{n_u} \\ p_{uc} \cdot (r - \frac{T}{2n_u}), & r > \frac{T}{n_u}. \end{cases} \quad (38)$$

□

B.5 Influencing factors of p_{uc}

Our experimental results indicate that the p_{uc} value is typically less than 0.01, meaning that the waiting time for DIMP does not exceed 1% of SISA. We can also qualitatively analyze p_{uc} based on the characteristics of the model:

1. The higher the model accuracy, the lower p_{uc} . This is because the lower the model accuracy, the more random the prediction results, and each constituent model may give different prediction results; while the higher the model accuracy, the more likely it is that the prediction results of all constituent models are the correct label. According to the definition of fine-grained certification, the higher the consistency among constituent models, the more likely it is to obtain a certified prediction result.

2. The longer the single retraining duration r , the higher p_{uc} . In the case of the same density of unlearnt requests, a larger r usually results in more constituent models being retrained at the same time, which obviously leads to a higher probability of uncertified prediction results.

C The Overall Framework of ERASER

Algorithm 1 summarizes the training and inference with certified inference consistency check in ERASER, where the unlearning execution is omitted since it heavily depends on design options.

Algorithm 1 ERASER: training and inference with certified inference consistency check

Input: Training dataset $\mathcal{D} = \{\mathbf{x}_1, \dots, \mathbf{x}_N\}$

Training:

- 1: Randomly divides \mathcal{D} into K shards $\mathcal{S}_1, \dots, \mathcal{S}_K$
- 2: Train constituent model f_k on \mathcal{S}_k , for all $k \in [1, 2, \dots, K]$
- 3: Launch inference service with $F = \{f_1, \dots, f_K\}$

Inference and Unlearning Serving:

- 4: **for** $t \in [1, 2, \dots]$ **do**
- 5: **if** Receive an Unlearning Request $u = (i, 'Unlearn')$ **then**
- 6: Record it as a pending unlearning request
- 7: **else if** Receive an Inference Request $u = (\mathbf{z}, 'Inference')$ **then**
- 8: Inference with constituent models: $f_1^0(\mathbf{z}), \dots, f_K^0(\mathbf{z})$
- 9: Count: $Count_y^0(\mathbf{z}) := |\{k \in [K] | f_k^0(\mathbf{z}) = y\}|$.
- 10: **if** satisfy certified inference consistency condition **then**
- 11: Return $F(\mathbf{z}) := \arg \max_{y \in \mathbb{Y}} Count_y^0(\mathbf{z})$.
- 12: **else**
- 13: Halt
- 14: **end if**
- 15: **end if**
- 16: **end for**

Output:

D Extended Comparison for Variants of ERASER

In the following, regarding different design options, we provide an extended comparison for variants of ERASER.

Double Contexts for Immediate Unlearning with Postponed Certified Inference (DIMP). DIMP maintains both

the inference context and the unlearning context, choosing to execute unlearning requests immediately at the back-end. Inference requests with certified results will receive immediate responses, while uncertified requests will be postponed until the ongoing unlearning update is completed. This variant offers low inference latency at the cost of high computation overhead since each unlearning update can process only one unlearning request.

Single Context for Uncertification-Triggered Unlearning with Postponed Certified Inference (SUTP). SUTP maintains a single context at a time and accumulates unlearning requests until an inference request fails to satisfy the certified inference consistency condition. Instead of updating immediately, constituent models corresponding to unlearning requests are placed in an unlearning waiting list. Once uncertification occurs, the server switches to the unlearning context and executes the unlearning update. Uncertified prediction requests will be postponed until the server completes the unlearning update and switches back to the inference context, as well as the inference requests that arrive during the unlearning context. This variant saves computation overhead compared to DIMP, but at the cost of increased inference latency.

Double Contexts for Uncertification-Triggered Unlearning with Postponed Certified Inference (DUTP). DUTP differs from SUTP by maintaining both the inference and unlearning contexts. In this variant, inference requests that arrive during unlearning execution receive immediate responses if the inference result is certified. Only uncertified inference requests are postponed. DUTP reduces inference latency compared to SUTP while consuming more resources by maintaining double contexts simultaneously.

Single Context for Threshold-Triggered Unlearning with Uncertified Inference (STTU). STTU maintains a single context at a time and accumulates unlearning requests until the ratio of inference requests that fail to satisfy the certified inference consistency condition exceeds a threshold. Uncertified inference results within the predetermined threshold are provided immediately. Once the ratio exceeds the threshold, the server switches to the unlearning context and executes the unlearning update. The request that triggers the update and newly arrived inference requests during the update must wait for the context switch. This variant reduces the frequency of unlearning updates, decreasing computation overhead. However, a predetermined small ratio of inference requests will receive uncertified prediction results, introducing potential privacy risks.

Double Context for Threshold-Triggered Unlearning with Uncertified Inference (DTTU). DTTU differs from STTU by maintaining both the inference and unlearning contexts, reducing inference latency by responding to inference requests during unlearning updates.

Single Context for Threshold-Triggered Unlearning with Postponed Certified Inference (STTP). STTP shares the

same choices as STTU for Option I and Option II. However, this variant stores uncertified inference requests in an inference waiting list rather than providing uncertified predictions immediately. These requests are postponed and re-processed during the next unlearning update. STTP guarantees that every inference will receive a certified prediction. Furthermore, the ratio of uncertified requests resets to zero since every uncertified request is reprocessed after an unlearning update, making it take longer to trigger the next unlearning update. This means STTP saves more computation overhead than STTU, but at the cost of higher inference latency due to uncertified inference requests waiting for reprocessing.

Double Context for Threshold-Triggered Unlearning with Postponed Certified Inference (DTTP). DTTP differs from STTP by maintaining double contexts and reducing inference latency by responding to inference requests during unlearning updates.

We provide three options that can be combined to create a total of 12 variants, but not all variants are practical. For example, when choosing A or B in Option II, uncertified inference requests only need to wait for the completion of the ongoing unlearning update to receive certified results. In this case, it is not reasonable for the server to provide uncertified predictions immediately. Only when choosing C in Option II, as uncertified inference requests must wait for the next unlearning update that may start after a long time, is it reasonable to significantly reduce inference latency at the cost of a small privacy risk. Additionally, SISA with an unlearning-request-first strategy, as described in Sec.3.2, can be viewed as a variant with Options B-B-B.

E Malicious Requests and Mitigation

In addition to the toy attacks on security and privacy in Sec.3.2, we present two more attacks that can be launched by queriers and data owners through malicious inference and unlearning requests, respectively, aiming to consume the server’s computational resources and slow down its response time.

E.1 Malicious Inference Requests: Hard-to-Classify Inferences

Attack. In the first attack, we consider malicious inference requests from adversarial queriers, whose goal is to increase the overall inference latency by triggering the unlearning mechanism more frequently. When an inference request cannot satisfy the certified inference consistency condition, it may trigger the unlearning-update mechanism and halt subsequent inference requests until the unlearning-update finishes. As a result, adversarial queriers submit inference samples that are hard to classify. These samples are more likely to yield different prediction results across constituent models, ultimately increasing the likelihood of uncertified inference consistency.

In particular, we consider malicious inference requests to contain random noise data, which increases the inference latency for normal queries by triggering the unlearning mechanism more frequently.

Mitigation. Two potential strategies for the server to mitigate the threat posed by hard-to-classify inference requests: detection before inference and discard after inference. For the former, the server screens all inference samples to detect whether they are malicious based on a predefined detection rule. In the concrete example above, the server detects whether the inference sample is random noise data and stops predicting if that is the case. For the latter, the server still runs the inference process for the sample but discards it if the confidence score (e.g., softmax score) of the prediction result is exceptionally low, therefore avoiding triggering the unlearning mechanism.

E.2 Malicious Unlearning Requests: Scattered Unlearnings

Attack. In the second attack, we consider malicious unlearning requests from adversarial data owners, whose goal is to waste the server’s computation on unlearning mechanism. The server saves more computation on unlearning mechanism if more pending unlearning requests are processed all at once by a single unlearning execution. As a result, adversarial data owners collude and coordinate with each other to submit unlearning requests that are more scattered in timestamps and shards. This way, they increase the chance that a later unlearning request just arrived when the most recent unlearning execution finishes, which however could have been processed together with an earlier unlearning request. In particular, we consider malicious unlearning requests to revoke data lying at each shard in a rolling manner, therefore being more scattered in both timestamps and shards. That is, the i -th unlearning request from the adversarial data owners corresponds to the $i \bmod K$ -th shard, where K is the total number of shards.

Mitigation. To mitigate the threat posed by scattered unlearning requests, The server must prevent the attackers from establishing the correspondence between their training samples and the assigned shards. Thus the server could shuffle the training dataset and randomly divides it into shards according to non-fixed hash functions. In this way, the adversary would have difficulty determining the location of their data.

F Additional Experiments

F.1 Model Accuracy

The performance of methods varies across different datasets. Firstly, the larger the model, the longer the unlearning update takes, leading to longer AWT. Secondly, for easily classifiable datasets or models with higher accuracy, such as Purchase and Mnist, different constituent models are more likely to

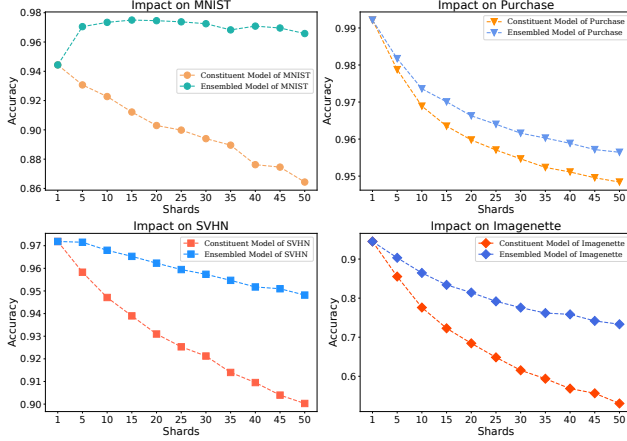


Figure 8: Evaluation on Model Accuracy with Different Number of Shards.

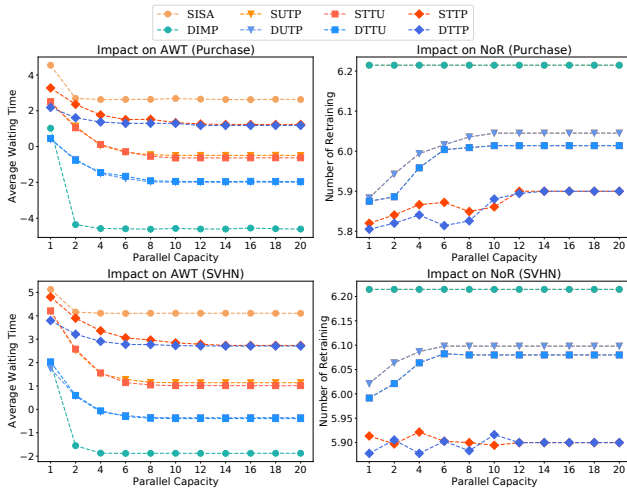


Figure 9: Evaluation on Parallel Capacity.

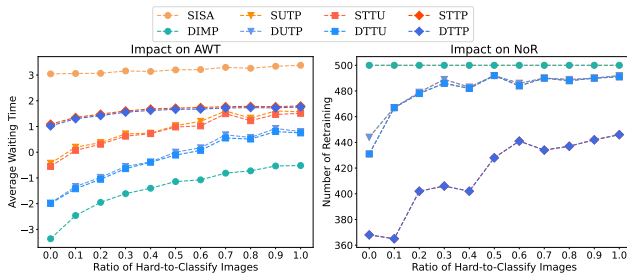


Figure 10: Evaluation on Hard-to-Classify Inference Requests.

give consistent predictions, resulting in a lower probability of uncertified predictions. However, for Resnet-18 trained on ImageNette, which has lower accuracy, uncertified prediction results are more likely, triggering more frequent unlearning

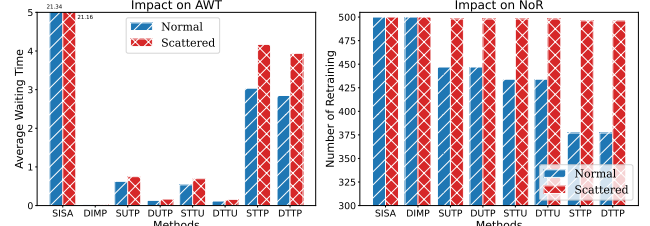


Figure 11: Evaluation of Scattered Unlearning Requests.

updates and longer waiting times. We report the model accuracy with varying numbers of shards in Figure 8. The accuracy of all models decreases as the number of shards increases.

F.2 Evaluation of Parallel Capacity

Considering the limited computing resources available for the server to retrain constituent models, we set a parallel capacity parameter representing the maximum number of constituent models that the server can retrain simultaneously. The experimental results are shown in Figure 9.

The inference latency for all methods is negatively correlated with parallel capacity. However, once the parallel capacity exceeds half the number of constituent models, further increasing the parallel capacity has minimal effect. This is because when the number of constituent models in the unlearning waiting list exceeds half of the total, all prediction results must be uncertified. In this case, the unlearning update will start quickly, regardless of the method used. Therefore, it is rare for the server to have to retrain more than half of the constituent models simultaneously.

The NoR for most methods increases with the parallel capacity. This is because when the unlearning update is triggered, it is usually sufficient to retrain only part of the constituent models in the unlearning waiting list to make the prediction results certified. However, if the parallel capacity exceeds the number of models needing retraining, a few more models in the unlearning waiting list will be retrained in advance to fully utilize the server’s computing resources.

F.3 Malicious Inference and Unlearning Requests

To verify the effectiveness of the proposed malicious inference and unlearning requests, we conduct experiments on the Mnist dataset, using the same parameter settings as in Sec.6.2.

Hard-to-Classify Inference Requests. In this experiment, we replace the test data of some inference requests with random noise images of the same size. The replacement ratio ranged from 10% to 100%. The experimental results in Figure 10 demonstrate that submitting randomly generated inference requests is more likely to yield uncertified prediction results, which will trigger unlearning updates and increase inference

latency. This attack can be mitigated by detecting and rejecting such inference requests.

Scattered Unlearning Requests. We compare the performance of ERASER with normal and scattered unlearning requests. The experimental results in Figure 11 reveal that scattered unlearning requests can increase inference latency and cause computation overhead to approach the theoretical upper limit. Defending against such attacks can be achieved by shuffling the training dataset to prevent attackers from knowing the correspondence between data and shard indexes.